

**STABILITY CONSTANTS FOR GLYCINE
UNDER HYDROTHERMAL CONDITIONS
USING COLORIMETRIC INDICATORS**

by

© Christopher M. Collins

A dissertation submitted to the
Department of Chemistry
in partial fulfilment of the requirements for the degree of
Bachelor of Science (Honours)

in

The Department of Chemistry
and
The Department of Computer Science
Faculty of Science
Memorial University of Newfoundland

April, 2001

ABSTRACT

Hydrothermal conditions are known to occur at deep ocean hydrothermal vents, where thermophilic life is hypothesized to exist. Amino acids under hydrothermal conditions are of interest as knowledge of their properties will contribute to theories of hydrothermal vents as possible sources for the origin of life. Amino acids, such as glycine, are zwitterions and have both basic and acidic dissociation reactions in solution. Glycine is known to have a limited stability under hydrothermal conditions (Clarke, Ph.D. Thesis, Memorial University of Newfoundland, 2000), thus stability constants for these reactions are not known above 423 K. In this work a UV-visible spectrophotometer and flow system with the colorimetric indicators acridine, 2-naphthol, and 2-naphthoic acid, developed by Xiang and Johnston (*J. Sol. Chem.* **26**, 13-30, 1997; *J. Phys. Chem.* **98**, 7915-7922) and Ryan *et al.* (*J. Phys. Chem.* **101**, 1827-1835, 1997) are used with buffer solutions of glycine in the determination of stability constants for the isocoulombic dissociation reactions from 348 to 548 K. Stopped-flow experiments were used to confirm that glycine and acridine are stable for the time-scale required for measurements in the flow cell. The van't Hoff equation is used to express a temperature dependence for the acid/base stability constants of glycine. The first experimentally determined acid/base stability constants for glycine at temperatures above 423 K are reported in this work.

ACKNOWLEDGEMENTS

There are many people who have assisted this project and my completion of my degree as the first student in the joint B.Sc. Honours program in Computer Science and Chemistry at Memorial University of Newfoundland:

First and foremost, my mentor and supervisor, Dr. Peter Tremaine, who has given his unfailing support and encouragement throughout my university education. From first year until this landmark, Dr. Tremaine has been an invaluable teacher and friend in all my endeavours both inside and outside the chemistry lab.

Dr. Rodney Clarke previously included preliminary work using colorimetric indicators for study of α -alanine in his Ph.D. thesis. I am thankful to Rodney for his guidance.

Dr. Paul Gillard, Head of the Department of Computer Science, for being my academic advisor throughout my time in the computer science program.

Dr. Liliana Trevani, Dr. Richard Bartholomew, and Ms. Linda Thompson of the Department of Chemistry, Mr. Randy Thorne of the machine shop, and my other colleagues in the hydrothermal chemistry group for advice and assistance in the laboratory. Ms. Jenene

Roberts, a fellow honours student in the Department of Chemistry, was a great help while I was learning about the experimental setup is always resourceful when solving equipment problems.

My parents, Mervin and Christina Collins, who sacrificed much to give me opportunities few people are afforded, and who have tolerated my short fuse during the years of long hours of study. My sister, Lesley Collins, who is just starting her program at Memorial and is always available for comic relief. Finally, my grandparents Paul and Mary McDonald, who have provided many entertaining lunch breaks during this honours project. Their love and support is an important source of strength in my research and extracurricular activities.

TABLE OF CONTENTS

Abstract	ii
Acknowledgements	iii
Table of Contents	v
List of Figures	vii
List of Tables	viii
List of Symbols and Abbreviations	ix
Chapter 1 Introduction	1
1.1 The Importance of Amino Acids Under Hydrothermal Conditions	1
1.2 Amino Acid Chemistry in Aqueous Solutions	3
1.3 Thermodynamic Data in the Literature	5
1.3.1 Data at Low Temperatures	5
1.3.2 Extrapolation of Room Temperature Stability Constants to Hydrothermal Conditions	5
1.4 Colorimetric Indicators	8
1.4.1 Colorimetric Indicators for Hydrothermal pH Measurement ...	8
1.4.2 Indicator Ranges vs. Predicted Stability Constants of Glycine .	12
Chapter 2 Experimental	16
2.1 Materials	16
2.2 Apparatus	18

2.3	Methods	22
2.3.1	Flow Experiments	22
2.3.2	Stopped Flow Experiments	25
Chapter 3	Results and Discussion	27
3.1	Stability Constant K_1	27
3.1.1	Measurements Using Acridine	27
3.1.2	Representation of Temperature Dependence of $\ln K_1$	32
3.2	Stability Constant K_2	34
3.2.1	Measurements Using 2-Naphthol	34
3.2.2	Measurements Using 2-Naphthoic Acid	39
3.2.3	Representation of Temperature Dependence of $\ln K_2$	41
3.3	Stopped Flow Experiments	43
Chapter 4	Conclusion	46
Chapter 5	Bibliography	48

LIST OF FIGURES

1.2.1	Glycine	3
1.4.1.1	Colorimetric indicators	12
1.4.2.1	Predicted glycine pK_1 and acridine indicator range	14
1.4.2.2	Predicted glycine pK_2 and corresponding indicator ranges	15
2.2.1	Titanium flow cell schematic	19
2.2.2	High pressure flow system schematic	20
3.1.1.1	Absorbance spectra of acridine	30
3.1.1.2	Fitting of spectra of acridine in buffer solution	31
3.1.2.1	Temperature dependence of pK_1	33
3.2.1.1	Absorbance spectra of 2-naphthol	37
3.2.1.2	Fitting of spectra of 2-naphthol in buffer solution	38
3.2.2.1	Absorbance spectra of 2-naphthoic acid	40
3.2.3.1	Temperature dependence of pK_2	42
3.3.1	Change in absorbance of acridine in glycine buffer with time	44
3.3.2	Change in absorbance of acridine in triflic acid with time	45

LIST OF TABLES

1.3.2.1	Reference temperature and pressure thermodynamic data for glycine . . .	7
2.3.1	Wavelengths ranges used to fit spectra of indicators in buffer solution .	24
3.1.1.1	Experimentally determined pK_1 vs. temperature	29
3.1.2.1	Low temperature pK_1 values from Wang <i>et al.</i> (1996)	32
3.1.2.2	Van't Hoff fit parameters for $\ln K_1$ vs. temperature	34
3.2.1.1	Experimentally determined pK_2 vs. temperature	36
3.2.3.1	Van't Hoff fit parameters for $\ln K_4$ vs. temperature	41

LIST OF SYMBOLS AND ABBREVIATIONS

$\Delta_r C_p^\circ$	change in partial molar heat capacity over a reaction
$\Delta_r H_{T,p}^\circ$	standard partial molar enthalpy at T, p
$\Delta_r H_{T_r, p_r}^\circ$	standard partial molar enthalpy at T_r, p_r
ϵ	absorptivity
ϵ	dielectric constant
λ	wavelength
2-Nap	2-naphthol (β -naphthol)
A	absorbance
A^-	deprotonated form of glycine
Ac	acridine
BNA	2-naphthoic acid (β -naphthoic acid)
f_i	fitting parameter i
H_2A^+	protonated form of glycine
HA°	neutral form of glycine
HA^\pm	zwitterionic form of glycine
HIn (HIn^+)	protonated form of colorimetric indicator (acridine)
I	ionic strength
In^- (In)	deprotonated form of colorimetric indicator (acridine)
K_i	stability constant of reaction i
m_i	molality of solute i
p	pressure
p_r	reference pressure (usually 0.1 MPa)
Q_w	dissociation constant of water in a solution of $I > 0$
R	universal gas constant; $R = 8.31451 \text{ J K}^{-1} \text{ mol}^{-1}$

T	temperature
T_r	reference temperature (usually 298.15 K)

CHAPTER 1 - INTRODUCTION

1.1 The Importance of Amino Acids Under Hydrothermal Conditions

Amino acids under hydrothermal conditions are of great interest to the chemical, geochemical, and biological fields as their properties are key to existence of thermophilic bacteria and theories of the origin of life at deep ocean hydrothermal vents.

Hydrothermal conditions refer to water constrained in its liquid form due to elevated pressures at temperatures above 100°C. These conditions occur in nature at deep ocean vents, located along undersea tectonic rifts and ridges. The first of these were discovered at the Galapagos Islands and along the East Pacific Rise (Spies *et al.*, 1980). The most extreme conditions have been found at vents, known as “black smokers”, on the East Pacific Rise near 21°N expelling “smokey black” water at temperatures exceeding 350°C and containing suspended metal sulfides. Since the discovery of deep ocean hydrothermal vents, which are classified into either Galapagos-type (~20°C) or sulfide-mound hot-water type (~375°C) vents by Spies *et al.* (1980), amino acids have been of intense interest and at the centre of theories about hydrothermal vents as locales for the origin of life on Earth.

As the high pressures, which permit the existence of liquid water at these elevated temperatures, counteract the destructive effects of high temperature on biochemical systems,

it is reasonable to question whether thermophilic life exists in these high-temperature environments. Several life forms, such as tube-worms and giant clams have been found to exist in the temperature gradient region surrounding vents.

It has been calculated by Miller and Bada (1988) that the entire ocean passes through hydrothermal vents every 10^7 years. Therefore, the processes that take place at these vents must be important to the overall organic profile of seawater. Miller and Bada report that hydrothermal vents destroy, rather than form, organic molecules such as amino acids. However, Shock (1992) has shown that less energy is required to form peptide bonds under hydrothermal conditions than at ocean surface conditions. Shock (1990) has reinterpreted the data of Miller and Bada (1988) to show that aqueous amino acids approach metastable equilibrium concentrations under hydrothermal conditions and that the thermodynamic stability of peptide bonds is not a limiting constraint on the maximum temperature which life can tolerate. Glycine was shown to be the predominant amino acid in the metastable equilibrium solution. Metastable equilibrium refers to a state at which the distribution of aqueous organic compounds represents a local energetic minimum, but not all the stable equilibrium species are present due to kinetic constraints.

Upper temperature limits for life are not currently known, and it has been shown that the high pressures experienced under hydrothermal conditions partially counteract the destructiveness of high temperature (Shock, 1990). Stetter (1982) has isolated anaerobic

bacteria that grow optimally at 105°C. Yanagawa and Kojima (1985) have reported the formation of stable microspheres containing peptide-like polymers made of amino acids at 250°C. Baross and Deming (1983) have reported successful culturing of thermophilic bacteria sampled from hydrothermal vent water at 250°C, although these results are vigorously disputed by Trent *et al.* (1984). Each of these studies lacks reliable, experimentally determined thermodynamic data, including stability constants for glycine, under the conditions of interest. Clarke (2000) has reported thermodynamic data and the first stability constants for α -alanine under hydrothermal conditions. The stability constants for glycine under hydrothermal conditions have not been reported. Therefore, an experimental investigation of these properties may contribute to our understanding of the extent to which microorganisms may thrive at high temperatures and pressures, and of the probability of deep ocean hydrothermal vents as a locale for the origin of life.

1.2 Amino Acid Chemistry in Aqueous Solutions

Amino acids exist in aqueous solutions as zwitterions - molecules with both positive and negative charge. Glycine, seen in Figure 1.2.1, is an example of an amino acid. These molecules can undergo association and dissociation into the protonated and deprotonated forms, respectively, as well as equilibrium between neutral and zwitterionic forms:

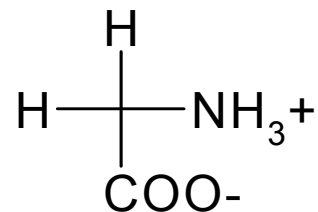


Figure 1.2.1:
Glycine zwitterion

$$\text{H}_2\text{A}^{\circ} \rightleftharpoons \text{HA}^{\pm} + \text{H}^+; K_1 = \frac{m_{\text{H}^+} m_{\text{HA}^{\pm}} \gamma_{\text{H}^+} \gamma_{\text{HA}^{\pm}}}{m_{\text{H}_2\text{A}^{\circ}} \gamma_{\text{H}_2\text{A}^{\circ}}} \quad (1.2.1)$$

$$\text{HA}^{\pm} \rightleftharpoons \text{A}^- + \text{H}^+; K_2 = \frac{m_{\text{A}^-} m_{\text{H}^+} \gamma_{\text{A}^-} \gamma_{\text{H}^+}}{m_{\text{HA}^{\pm}} \gamma_{\text{HA}^{\pm}}} \quad (1.2.2)$$

$$\text{HA}^{\circ} \rightleftharpoons \text{HA}^{\pm}; K_3 = \frac{m_{\text{HA}^{\pm}}}{m_{\text{HA}^{\circ}}} \quad (1.2.3)$$

$$\text{HA}^{\pm} + \text{OH}^- \rightleftharpoons \text{A}^- + \text{H}_2\text{O}; K_4 = \frac{m_{\text{A}^-} \gamma_{\text{A}^-}}{m_{\text{HA}^{\pm}} m_{\text{OH}^-} \gamma_{\text{HA}^{\pm}} \gamma_{\text{OH}^-}} \quad (1.2.4)$$

Here, the activity coefficients of the neutral species HA° and HA^{\pm} are assumed to be unity.

We have chosen to use the isocoulombic equilibrium constants, K_1 and K_4 , in this work, because the activity coefficient ratios $(\gamma_{\text{H}^+} / \gamma_{\text{H}_2\text{A}^{\circ}})$ and $(\gamma_{\text{A}^-} / \gamma_{\text{OH}^-})$ may be assumed to be near unity at the elevated temperatures and modest ionic strengths studied in this work. The equilibrium constant for reaction 1.2.2 can be calculated from the dissociation constant of water through the relationship:

$$K_2 = K_4 \mathcal{K}_w \quad (1.2.5)$$

Values for the dissociation constant of water,

$$\mathcal{K}_w = m_{\text{H}^+} m_{\text{OH}^-} \quad (1.2.6)$$

have been reported as a function of ionic strength at elevated temperatures by Sweeton *et al.* (1974). In the measurements described below, we have used buffer solutions with known molalities m_{A^-} , m_{HA^\pm} , and $m_{H_2A^+}$, and determined m_{H^+} with colorimetric indicators so that K_4 can be determined from the expression:

$$K_4 = \frac{m_{A^-} m_{H^+}}{m_{HA^\pm} Q_w} \quad (1.2.7)$$

We have also assumed that the stepwise ionization of the amino acid is additive, so that $K_3 = K_1 / K_2$, to assess whether the neutral species HA° is a significant species in our solutions.

1.3 Thermodynamic Data in the Literature

1.3.1 Data at Low Temperatures

The stability constants of glycine have been reported by Wang *et al.* (1996) up to 398 K. Experimental measurements of these properties at higher temperatures are not available.

1.3.2 Extrapolation of Room Temperature Stability Constants to Hydrothermal Conditions

In order to have an estimate of the stability constants at elevated temperatures and pressures, room temperature data was extrapolated using standard thermodynamic relationships. This

information is useful in deciding which indicator has a K_{in} best suited for use with glycine buffer solutions at each temperature. The method of Clarke (2000) was adopted. For a given constant pressure p , the temperature dependent equilibrium constant $K_{T,p}$ can be expressed in terms of the enthalpy of reaction:

$$\left(\frac{\delta \ln K_{T,p}}{\delta T} \right)_p = \left(\frac{\Delta_r H_{T,p}^o}{RT^2} \right) \quad (1.3.2.1)$$

where R is the universal gas constant. The standard partial molar enthalpy of reaction is expressed in the following equation:

$$\left(\frac{\delta \Delta_r H_{T,p}^o}{\delta T} \right) = \Delta_r C_p^o \quad (1.3.2.2)$$

where $\Delta_r C_p^o$ is the standard partial molar heat capacity of reaction at T and p . Then, if we assume $\Delta_r C_p^o$ to be temperature independent, integration gives:

$$\Delta_r H_{T,p}^o = \Delta_r H_{T_r,p_r}^o + \left(\Delta_r C_p^o \right) (T - T_r) \quad (1.3.2.3)$$

where $\Delta_r H_{T_r,p_r}^o$ is the standard partial molar enthalpy of reaction at a reference temperature T_r (usually 298.15 K) and a reference pressure p_r (usually 101.325 kPa). Substituting equation 1.3.2.3 into equation 1.3.2.1 yields:

$$\left(\frac{\delta \ln K_{T,p}}{\delta T} \right)_p = \left(\frac{\Delta_r H_{T_r,p_r}^o + \left(\Delta_r C_p^o \right) (T - T_r)}{RT^2} \right) \quad (1.3.2.4)$$

Equation 1.3.2.4 is integrated to yield:

$$\ln K_{T,p} = \ln K_{T_r,p_r} + \left(\frac{\Delta_r H_{T_r,p_r}^{\circ}}{R} \right) \left(\frac{1}{T_r} - \frac{1}{T} \right) + (\ln T - \ln T_r) \left(\frac{\Delta_r C_p^{\circ}}{R} \right) - \left(\frac{\Delta_r C_p^{\circ} (T - T_r)}{RT} \right) \quad (1.3.2.5)$$

The effects of pressure are negligible in comparison to temperature effects. Equation 1.3.2.5 is used with the thermodynamic data of Table 1.3.2.1 to predict hydrothermal stability K_1 and K_4 for the isocoulombic reactions (where the heat capacity change is minimized). The relationship $K_2 = K_4 @K_w$ can then be used to recover K_2 , using K_w calculated from the expression for K_w at temperature T given by Sweeton *et al.* (1974).

Table 1.3.2.1 Data for Glycine at $T_r = 298.15$ K, $p_r = 101$ kPa for equation 1.3.2.5

Thermodynamic Parameter	Value of Parameter	Source
$\ln K_w$	-32.228	Sweeton <i>et al.</i> (1974)
$)_{rw}H^{\circ} / (J \text{ mol}^{-1})$	-55840	Atkins (1990)
$)_{rw}C_p^{\circ} / (J \text{ K}^{-1} \text{ mol}^{-1})$	223.8	Atkins (1990)
$\ln K_1$	-5.4003	Wang <i>et al.</i> (1996)
$\ln K_2$	-22.515	Martell and Smith (1974)
$\ln K_4$	9.713	$(\ln K_2 - \ln K_w)$
$)_{r1}H^{\circ} / (J \text{ mol}^{-1})$	3921.3	Wang <i>et al.</i> (1996)
$)_{r2}H^{\circ} / (J \text{ mol}^{-1})$	44400	Martell and Smith (1974)
$)_{r4}H^{\circ} / (J \text{ mol}^{-1})$	-11500	$)_{r2}H^{\circ} +)_{rw}H^{\circ}$
$)_{r1}C_p^{\circ} / (J \text{ K}^{-1} \text{ mol}^{-1})$	-117.84	Wang <i>et al.</i> (1996)

$\Delta_r C_p^\circ / (\text{J K}^{-1} \text{mol}^{-1})$	72.3	Balakrishnan (1988)
$\Delta_r C_p^\circ / (\text{J K}^{-1} \text{mol}^{-1})$	296.1	$\Delta_r C_p^\circ + \Delta_{rw} C_p^\circ$

1.4 Colorimetric Indicators

1.4.1 Colorimetric Indicators in Hydrothermal pH Measurement

Traditional pH measurement under hydrothermal conditions is a slow process using an electrode (MacDonald *et al.*, 1992). Since it has been shown (Vallentyne, 1964) that glycine has a half life (concentration decreases by one half) in solution at 573 K of 1.4-2.1 hours, the use of electrodes to measure pH at these conditions is not feasible. Clarke (2000) has reported the successful use of a high pressure flow system and commercial UV-visible spectrophotometer to make rapid (1-2 min) measurements of the pH of solutions of " - alanine under hydrothermal conditions. The same method should be applicable to glycine.

Colorimetric indicators have recently been developed (Ryan *et al.*, 1997; Xiang and Johnston, 1997; Xiang and Johnston, 1994) which have markedly different UV spectra in acidic and basic solution. These compounds are especially applicable to study of amino acid dissociation, as amino acids do not absorb in the wavelength regions of interest. The indicator spectrum in a buffer solution is then expected to be a linear combination of the spectra of the acidic and basic forms of the indicator, yielding pH in short order.

The dissociation of the indicator can be expressed as:



Note that for the indicator acridine, the indicator forms are actually HIn^+ and In . The notation of HIn and In^- will be used throughout this work to represent any indicator in acid or base respectively.

The concentration m_{H^+} may then be obtained, neglecting activity coefficients (Xiang and Johnston, 1997), using the expression:

$$m_{\text{H}^+} = \frac{K_{\text{In}} m_{\text{HIn}}}{m_{\text{In}^-}} \quad (1.4.1.2)$$

The molarity ratio used in spectroscopy can be considered equal to the molality ratio if the density ratio is assumed to be unity. At a given temperature and pressure, the absorbance $A(\mathcal{B})$ of the indicator is given by the Beer-Lambert law, which here is expressed in terms of molalities as all solutions for this work were prepared by mass. For a solution of indicator in acid, the indicator will exist entirely in the HIn form and the absorbance is given by:

$$A(\lambda) = m_{\text{HIn}} \varepsilon_{\text{HIn}}(\lambda) \quad (1.4.1.3)$$

where $A(\mathcal{B})$ is the absorbance at wavelength \mathcal{B} , m_{HIn} is the molality of indicator in the protonated form in solution, and $\varepsilon_{\text{HIn}}(\mathcal{B})$ is the absorptivity of HIn at the wavelength \mathcal{B} . This

expression neglects the path length term of the Beer-Lambert law as the path-length for the light does not change in this work and can be incorporated into the constant absorptivity. For a basic solution the indicator will exist entirely in the In^- form and the absorbance is given by:

$$A(\lambda) = m_{\text{In}^-} \varepsilon_{\text{In}^-}(\lambda) \quad (1.4.1.4)$$

where $A(\mathcal{S})$ is the absorbance at wavelength \mathcal{S} , m_{In^-} is the molality of indicator in the deprotonated form in solution, and $\mathcal{G}_{\text{In}^-}(\mathcal{S})$ is the absorptivity of In^- at the wavelength \mathcal{S} .

For a solution with pH in the indicator range ($\text{pK}_{\text{In}} \pm 1$), both HIn and In^- will be present in appreciable amounts and the expression for absorbance becomes a linear combination of the absorption of the protonated and deprotonated forms of indicator:

$$A(\lambda) = m_{\text{HIn}} \varepsilon_{\text{HIn}}(\lambda) + m_{\text{In}^-} \varepsilon_{\text{In}^-}(\lambda) \quad (1.4.1.5)$$

Using equations 1.4.1.3 and 1.4.1.4 the values for \mathcal{G}_{HIn} and $\mathcal{G}_{\text{In}^-}$ can be determined at a given temperature and pressure. The absorbance for a solution containing both HIn and In^- will then have absorbance which is a function of the known absorptivities and the molalities of HIn and In^- .

The pH is then calculated from equation 1.4.1.2, and the temperature dependent value for K_{In} , which has been determined for a number of hydrothermally stable colorimetric indicators. Acridine, 2-naphthoic acid, and 2-naphthol, shown in Figure 1.4.1, have been

studied by Ryan *et al.* (1997), Xiang and Johnston (1997), and Xiang and Johnston (1994), respectively. These were used in this work as they have suitable values of K_{In} for use with glycine buffer solutions (see Figures 1.4.2.1, 1.4.2.2).

The equilibrium constant for acridine $K_{acridine}$ was measured at a pressure of 24.13 MPa and 298.15 K # T # 653.15 K (Xiang, 1996; Ryan *et al.*, 1997). $K_{acridine}$, expressed as a function of temperature T and temperature-dependent solvent dielectric constant \mathcal{G} is:

$$\ln K_{acridine} = -12.43 - 3663.04 \left(\frac{1}{T} - \frac{1}{T_r} \right) - \left(\frac{15874.31}{T} \right) \left(\frac{1}{\varepsilon} - \frac{1}{\varepsilon_r} \right) \quad (1.4.1.6)$$

where $T_r = 298.15$ K is the reference temperature and $\mathcal{G} = 78.38011$ is the dielectric constant of water at T_r .

The equilibrium constant for 2-naphthoic acid $K_{2-naphthoic}$ was measured at 34.46 MPa and 298.15 K # T # 673.15 K (Xiang and Johnston, 1997) and is expressed as a function of temperature T and the density of water D_w :

$$\log K_{2-naphthoic} = -13.553 + \left(\frac{7.824 \cdot 10^3}{T} \right) - \left(\frac{1.706 \cdot 10^6}{T^2} \right) + \left(\frac{6.318 \cdot 10^7}{T^3} \right) + k \cdot \log \rho_w \quad (1.4.1.7a)$$

where

$$k = -19.193 + \left(\frac{1.974 \cdot 10^4}{T} \right) - \left(\frac{13.336 \cdot 10^4}{T^2} \right) \quad (1.4.1.7b)$$

The equilibrium constant for 2-naphthol $K_{2\text{-naphthol}}$ was measured at 34.5 MPa and 298.15 K # T # 673.15 K (Xiang and Johnston, 1994) and is expressed as a function of temperature T and the density of water D_w :

$$\log K_{2\text{-naphthol}} = -4.186 - \left(\frac{2.822 \cdot 10^3}{T} \right) + \left(\frac{6.245 \cdot 10^5}{T^2} \right) - \left(\frac{8.355 \cdot 10^7}{T^3} \right) + k \cdot \log \rho_w \quad (1.4.1.8a)$$

where

$$k = 7.170 + \left(\frac{3.153 \cdot 10^3}{T} \right) + \left(\frac{9.54 \cdot 10^4}{T^2} \right) \quad (1.4.1.8b)$$

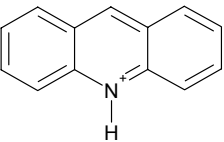
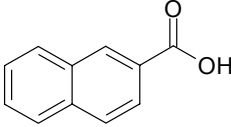
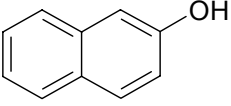
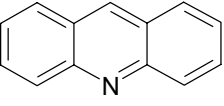
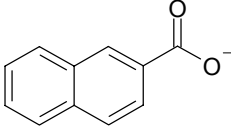
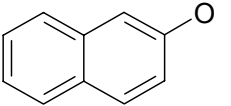
	acridine	2-naphthoic acid	2-naphthol
Indicator in acid			
Indicator in base			

Figure 1.4.1.1 Colorimetric Indicators

1.4.2 Indicator Ranges vs. Predicted Stability Constants of Glycine

The measurement range of pH using a given indicator is $\text{pK}_{\text{In}} \pm 1$, which is the range in which there are measurable amounts of both the HIn and In^- forms of indicator in solution. The values of pK_1 predicted for glycine using equation 1.3.2.5 are combined with an indicator range for acridine calculated with equation 1.4.1.6 and the resulting predicted range of possible measurement is plotted in Figure 1.4.2.1. The values of pK_2 predicted using equation 1.3.2.5 are combined with indicator ranges calculated with equation 1.4.1.7 and 1.4.1.8 for 2-naphthoic acid and 2-naphthol respectively and the resulting predicted ranges of possible measurement are plotted in Figure 1.4.2.2. The ranges at which the predicted pK values for glycine fall within the indicator range will be the main focus of this work.

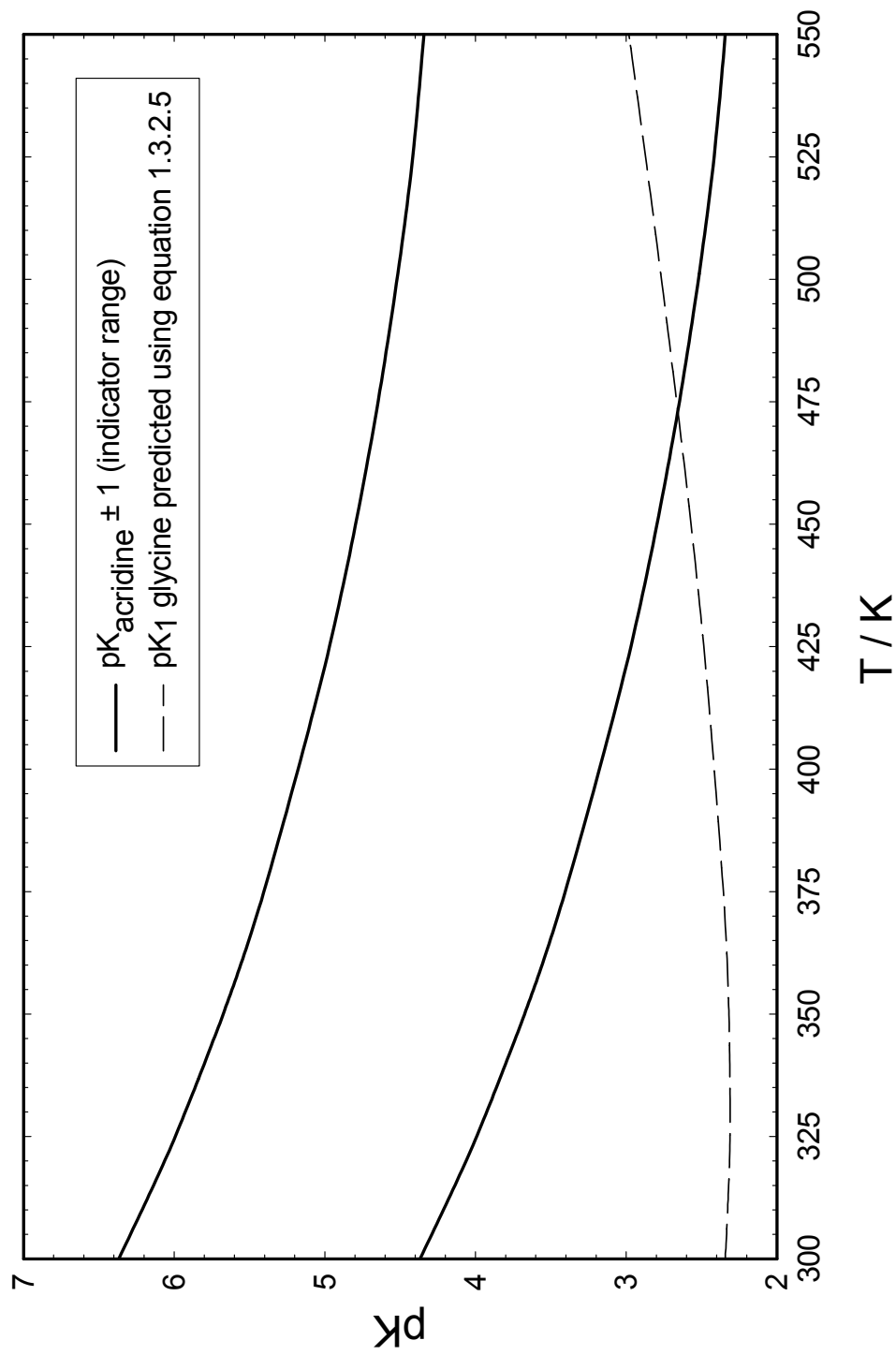


Figure 1.4.2.1 Predicted glycine pK₁ and acridine indicator range

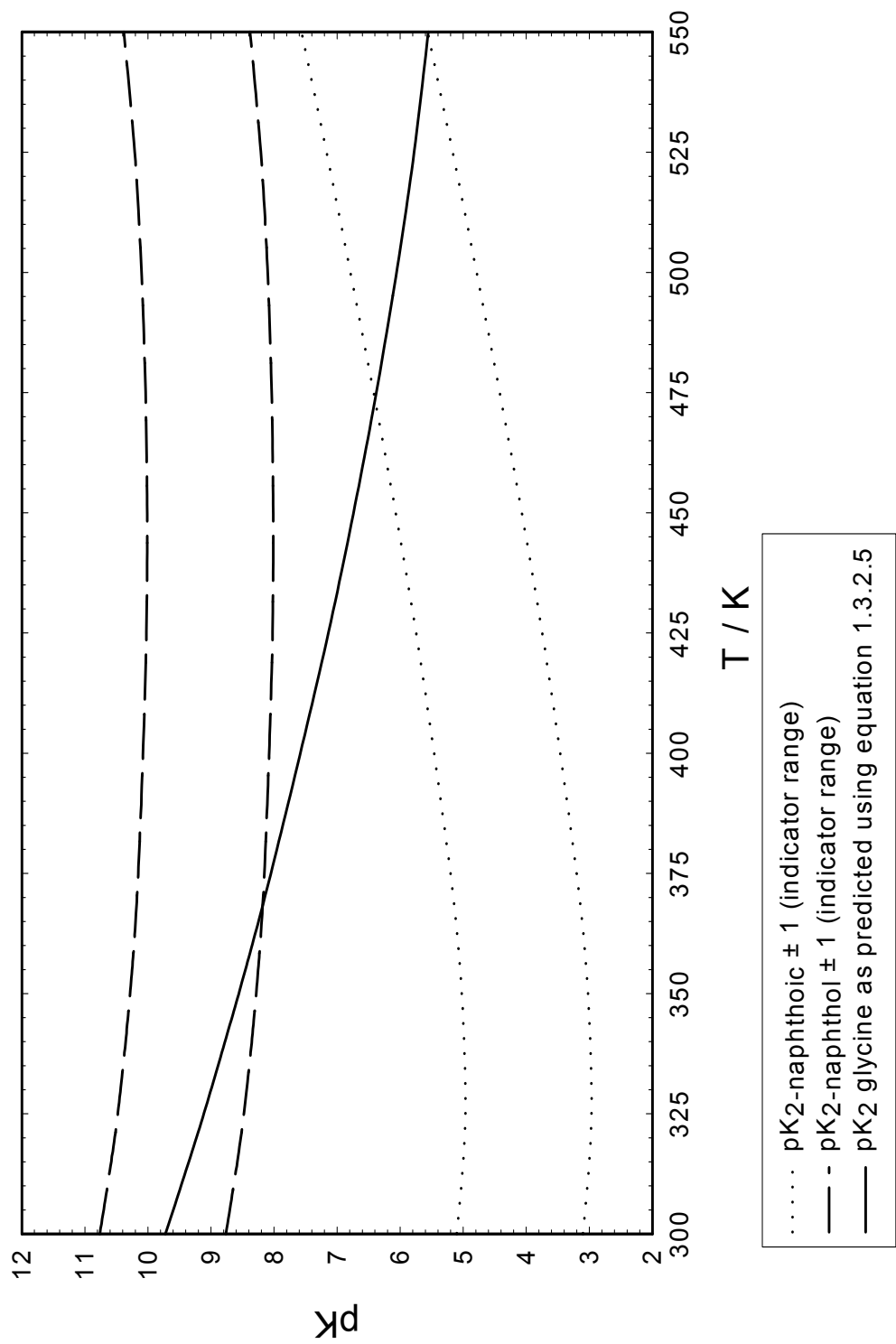


Figure 1.4.2.2 Predicted glycine pK₂ and corresponding indicator ranges

CHAPTER 2 - EXPERIMENTAL

2.1 Materials

Glycine was obtained from Aldrich (Assay 99+%). Before use, Rodney Clarke recrystallized the glycine according to the method of Perrin and Amarego (1988):

“Glycine was dissolved in a minimum amount of hot water ($T = 343 \text{ K}$). The resulting solutions were filtered while hot to remove any insoluble material. Hot ethanol ($T = 333 \text{ K}$) was slowly added to the filtrate until a 60/40 ethanol to water ratio was obtained. The resulting precipitate was allowed to digest for five hours at which time the white solids were collected and washed with cold water followed by cold ethanol. The purified glycine was dried under vacuum, over Drierite, for 120 hours at room temperature.”

This recrystallized glycine was used in this work. Sodium hydroxide was obtained from Fisher Scientific as a certified 50% w/w solution. This was used to prepare stock solutions of sodium hydroxide which were standardized by triplicate pH titration against potassium hydrogen phthalate (Analar, Analytical Reagent) using phenolphthalein as indicator. Trifluoromethanesulfonic (triflic) acid was obtained from Alfa Aesar (Assay 99%). This was used to prepare stock solutions of triflic acid which were standardized by triplicate pH titration against tris(hydroxymethyl)aminomethane (Aldrich, Assay 99.9+%) using methyl red as indicator. Buffer solutions of glycine were prepared for buffer ratios of 0.1, 0.2, 0.5,

1.0, 2.0, 5.0, and 10.0 for both the acidic (K_1) and basic (K_2) dissociations of glycine. Stock solutions of glycine were prepared by mass by dissolving solid glycine in water. Appropriate amounts of either aqueous sodium hydroxide stock or aqueous triflic acid stock were used to prepare the buffers.

Acridine (Aldrich, Assay 97%), 2-naphthoic acid (Aldrich, Assay 98%), and 2-naphthol (Aldrich, Assay 98%) were used without further purification. Solutions of acridine in acid, base, or buffer were made to final acridine molality $\sim 6.0 \times 10^{-5} \text{ mol kg}^{-1}$. Solutions of 2-naphthol and 2-naphthoic acid were made to final 2-naphthol molality $\sim 1.5 \times 10^{-4} \text{ mol kg}^{-1}$. These concentrations need not be exact, but the molalities given were found to give good absorbance levels for the apparatus used in this work. These indicators are light sensitive when in solution (Clarke, 2000; Ryan *et al.*, 1996; Xiang and Johnston, 1994; Xiang and Johnston, 1996) and insoluble in neutral water. Therefore, the following method was adopted for adding indicators to solution.

First, dissolve the indicator over several hours with stirring in either dilute stock triflic acid (acridine) or dilute stock sodium hydroxide (2-naphthoic acid, 2-naphthol), using a sealed, Nalgene bottle wrapped in aluminum. This solution is then diluted with more of the same stock solution and used as the first pH extremum for the experiment.

To obtain spectra of the second form of indicator, a sample of known mass of the stock

indicator solution is added to a known mass of either stock sodium hydroxide or stock triflic acid (whichever was not used to make the original indicator solution) so that there is an excess of the second stock solution. The UV absorption spectrum of the resulting solution is immediately collected, producing a spectrum for the other pH extremum.

Thirdly, the original stock indicator solution is neutralized and small, measured, aliquots of this neutralized solution are added to the prepared buffers. The buffer ratio is recalculated to account for any small excess of acid or base in the neutralized stock indicator solution. The resulting buffer solutions are used immediately.

Indicator stock solutions were made fresh each day and the above process carried out, using nalgene bottles covered with aluminum foil. Exposure to air was minimized by replacing the air in the top of the bottle with dry N₂ gas. Degassed, Nanopure (resistivity > 16 MS @m) water was used in the preparation of all solutions.

2.2 Apparatus

A high-temperature, high-pressure flow system was employed with a Cary 50 UV-visible spectrophotometer in this work. The flow system was developed by Trevani *et al.* (submitted) and is similar in concept to that developed by Chlistunoff *et al.* (1999). The system schematic is shown in Figures 2.2.1 and 2.2.2 and discussed below.

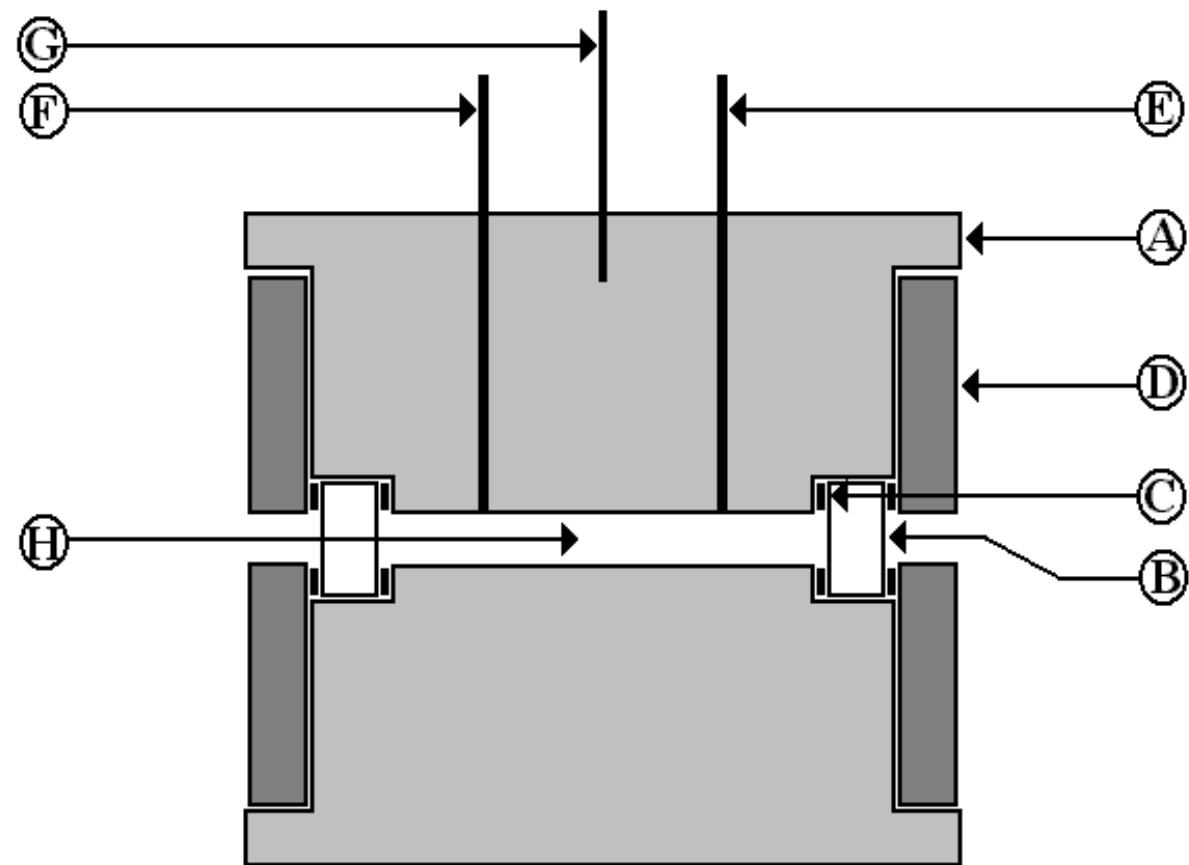


Figure 2.2.1 Schematic diagram of the spectroscopic flow cell. A, cylindrical titanium flow cell; B, sapphire window; C, Teflon washer; D, titanium disc; E, sample solution outlet; F, sample solution inlet; G, Chromega-Alomega thermocouple; H, sample compartment.

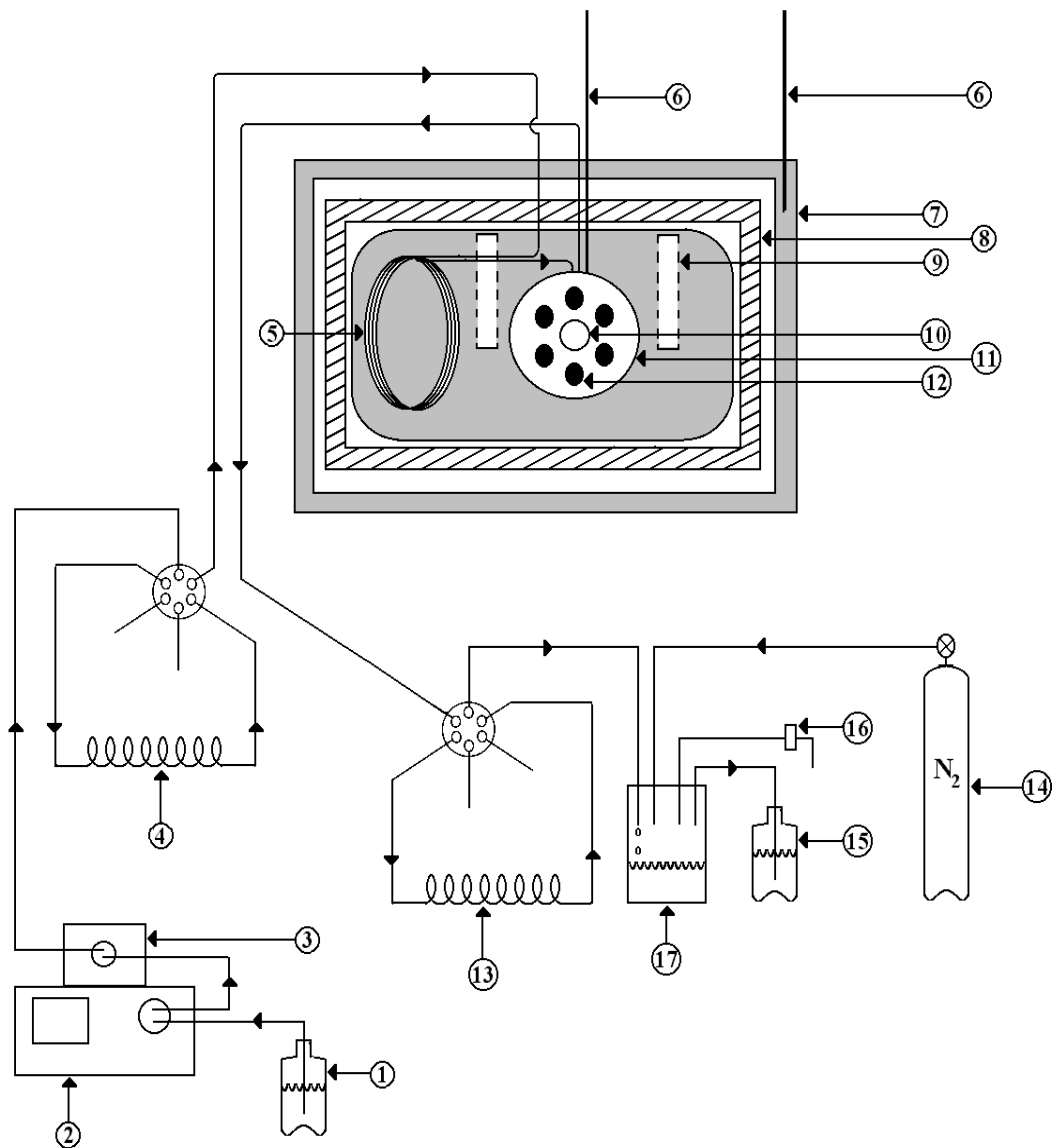


Figure 2.2.2 Schematic diagram of the spectroscopic flow system. 1, water reservoir; 2, Gilson 305 HPLC piston pump; 3, Gilson 805 manometric module; 4, injection loop; 5, preheater; 6, Chromega-Alomega thermocouple; 7, brass/aluminum housing; 8, ceramic insulation; 9, cartridge heater; 10, sapphire window; 11, titanium flow cell; 12, bolt; 13, sampling loop; 14, nitrogen cylinder; 15, reservoir for solution effluent; 16, back pressure regulator; 17, stainless steel reservoir.

The spectrum of a given solution is taken as the solution passes through a cylindrical titanium cell of volume 0.34 cm^3 . The cell is shown in Figure 2.2.1. A cylindrical channel was machined along the principal axis of a cylindrical piece of titanium. This central channel acts as the sample compartment in the cell. The cell is sealed against pressure effects and thermal expansion using Teflon washers cushioning both sides of sapphire windows. The optical path length is 1.72 cm. As can be seen in Figure 2.2.1, the solutions enter and exit the cell through 16 mm titanium tubing.

The titanium cell is mounted within two brass oven blocks. These blocks are heated using two Cromalux CIR-20203 (120 V, 200 W) cartridge heaters inserted into wells machined into the brass. A coil of titanium tubing is wound around a groove cut into the brass block and serves as a pre-heater. The temperature is controlled to $\pm 1 \text{ K}$ using an Omega CN7600 temperature controller and measured by a Chromega-Alomega thermocouple located in the body of the titanium cell. The brass oven and titanium cell are insulated by a ceramic casing (Rescor 310-COTRONICS). The entire ceramic case is placed into an aluminum and brass box, cooled by internal water circulation. The housing temperature is maintained near the ambient temperature of the coolant water and is monitored by a second Chromega-Alomega thermocouple located in the side of the brass-aluminum box as seen in Figure 2.2.2. The entire assembly is placed directly in the sample compartment of a Cary 50 UV-visible spectrophotometer and Cary Scan Application software is used for acquisition of spectra.

Flow through the system was volumetrically controlled by delivery of water using a Gilson 305 HPLC piston pump. A two-position six-port valve is used to direct the flow either directly to the cell or through an 18 cm³ PEEK (Upchurch Scientific) sample loop to force the sample into the flow cell. The sample solution is injected into the sample loop using a filling syringe and pre-pressurized before being opened for flow to the cell. Pressure is measured in the system using a Gilson 805 manometric module. The pressure in the system was maintained by a nitrogen filled cylinder and a Tescom model 26-1700 back-pressure regulator. Solutions are directed into a pressurized stainless steel waste reservoir upon exiting the flow cell. As can be seen in Figure 2.2.2, a second sample loop placed between the flow cell and the stainless steel reservoir can be used to collect a sample after running through the flow cell.

2.3 Methods

2.3.1 Flow Experiments

The values for the stability constants K_1 and K_2 of glycine were estimated using the method described in section 1.3.2. The temperatures at which the predicted stability constants of glycine lie within the indicator ranges of the indicators, as shown in Figures 1.4.2.1 and 1.4.2.2, were used as experimental conditions. Pressure was maintained at 4.5 MPa throughout the work.

In order to obtain good values for the absorptivities ϵ of the protonated and deprotonated forms of indicator, indicator concentrations were maintained at approximately the levels discussed in section 2.1. Solutions were prepared on the day of measurement. All spectra were later normalized to reflect indicator concentrations listed in section 2.1.

A baseline was measured at each temperature using water. Glycine, triflic acid, and sodium hydroxide do not absorb at any temperature in the wavelength region of interest, thus a water baseline is sufficient. Solutions of indicator in triflic acid, sodium hydroxide, and buffers of appropriate buffer ratio were run sequentially and the baseline reconfirmed several times during each day of experiments. Spectra were measured from $\lambda = 250\text{nm}$ to $\lambda = 500\text{nm}$, six times for each solution, using a constant flow rate of $0.2\text{ cm}^3\text{ min}^{-1}$. This gives a solution residency time of 1.7 min in the cell.

Using the spectra obtained at the extrema (indicator in triflic acid and indicator in sodium hydroxide), the spectra for the buffer solutions can be fit to obtain the ratio of protonated indicator HIn to deprotonated indicator In^- in solution. The fit equation is an extension of equation 1.4.1.5. The absorbances of the indicator in acid and in base can be used in place of absorptivities in equation 1.4.1.5 if either the molalities or absorbances are normalized for all solutions. As long as the spectra for the indicator in acid and indicator in base are normalized to the same indicator concentration, the normalization of molalities in buffer solutions can be left as part of the fitting parameters, allowing the total concentration of

indicator in buffer solutions to be unknown. The following equation was used to fit the spectra of buffer solutions over the wavelength ranges listed in Table 2.3.1:

$$A(\lambda)_{In,buffer} = f_1 A(\lambda)_{HIn,acid} + f_2 A(\lambda)_{In^-,base} \quad (2.3.1.1)$$

where f_1 and f_2 are fitting parameters equal to $m_{HIn,buffer} / m_{HIn,acid}$ and $m_{In^-,buffer} / m_{HIn,acid}$, respectively. f_1/f_2 gives the ratio of m_{HIn} / m_{In^-} independent of total indicator concentration in buffer.

Table 2.3.1 Wavelengths used to fit indicator in buffer spectra to equation 2.3.1.1

Indicator	acridine	2-naphthoic acid	2-naphthol
λ range used in fit	300 nm - 470 nm	270 nm - 400 nm	270 nm - 400 nm

The wavelength ranges were chosen to avoid absorption by the sapphire windows on the short wavelength end and to ensure that only wavelengths at which the protonated and deprotonated indicator forms absorb are considered. If the regions where the protonated and deprotonated forms of indicator have similar and very low absorbances are included, the fitting can converge to incorrect values.

Stability constants were calculated using m_{HIn} / m_{In^-} obtained from the fitting equation 2.3.1.1 to the indicator absorbance in buffer solution, and molalities of each form of glycine ($m_{H_2A^+}$ and m_{HA}) for K_1 or (m_{HA} and m_{A^-}) for K_2 in solution. The equilibrium molalities for glycine

were calculated using the initial composition of the buffer and any equilibrium shift as determined by using m_{H^+} of the buffer at T and p as calculated with equation 1.4.1.2. The following expressions, obtained from substitution of equation 1.4.1.2 into equation 1.2.1 and 1.2.7 give K_1 and K_4 respectively:

$$K_1 = \frac{K_{In} m_{HA^\pm} m_{HIn}}{m_{H_2A^+} m_{In^-}} \quad (2.3.1.2)$$

$$K_4 = \frac{K_{In} m_{A^-} m_{HIn}}{m_{HA^\pm} m_{In^-} Q_w} \quad (2.3.1.3)$$

where Q_w is the dissociation constant for water in a solution of given ionic strength. Values for Q_w were calculated using the equation of Sweeton *et al.* for each ionic strength of the buffer solutions. K_2 is then obtained using $K_4 = K_2 / K_w$. Uncertainties for each stability constant were calculated through propagation of experimental uncertainty and inclusion of ± 0.3 for each pK value to account for the assumption of unity activity ratio (Xiang and Johnston, 1996).

2.3.2 Stopped Flow Experiments

The stability of acridine was tested at 523.15 K for 30 minutes in aqueous glycine 1:1 $H_2A^+ : HA$ buffer and in triflic acid. The samples flowed through the cell at $0.2 \text{ cm}^3 \text{ min}^{-1}$

until thermal equilibrium was attained. The flow rate was slowly decreased so as to maintain a constant temperature. The flow was stopped and a series of spectra were measured every 1.5 min for 30 min.

CHAPTER 3 - RESULTS AND DISCUSSION

3.1 Stability Constant K_1

3.1.1 Measurements Using Acridine

Figure 3.1.1.1 compares the UV absorption spectra for protonated acridine, AcH^+ , in triflic acid and acridine, Ac , in sodium hydroxide with the spectrum of acridine in a buffer solution of glycine. Each UV-visible spectrum represents an average of six scans taken over a period of approximately 15 minutes. Experiments were carried out above 400 K, where it was expected that K_1 will lie within the indicator range. At each temperature, a baseline of the solution without acridine was subtracted from the spectrum of solution with acridine. The spectra shown for the indicators in acid or base can be thought of as the extrema of a continuum from one form to the other. Because acridine concentrations varied slightly each day of experimentation and between solutions, absorbance in these spectra was normalized to an acridine concentration of 6.0×10^{-5} mol kg^{-1} . Spectra of acridine in buffer solutions of glycine are expected to appear as intermediate between the extreme spectra. This result was seen and is illustrated in Figure 3.1.1.1.

Equation 2.3.1.1 was fit to the acridine in glycine spectra over the wavelength range 300 nm - 470 nm at intervals of 1 nm. The spectra for acridine in several glycine buffer solutions

of differing buffer ratios are shown as symbols in Figure 3.1.1.2. (For clarity, not all data points are shown). The results of the fitting equation 2.3.1.1 for each spectrum are plotted as solid lines in Figure 3.1.1.2. Values for K_1 were calculated for each buffer solution using equation 2.3.1.2. Figure 3.1.1.2 represents a single temperature of measurement; the same process was repeated for all temperatures which were used in this work. The experimentally determined values for buffer ratio, indicator ratio, and pK_1 with associated uncertainty appear in Table 3.1.1.1.

Table 3.1.1.1 Experimentally determined values of pK_1 as a function of temperature using acridine indicator in glycine buffer solutions

T / K	p / (MPa)	$R = m_{H_2A^+} / m_{HA^\pm}$	m_{AcH^+} / m_{Ac}	pK_1
423.2	4.5	0.1	2.89	2.73 ± 0.31
423.2	4.5	0.2	6.52	2.68 ± 0.32
423.2	4.5	0.9	40.7	2.47 ± 0.38
423.2	4.5	0.5	20.8	2.56 ± 0.35
473.2	4.5	0.09	0.911	2.83 ± 0.32
473.2	4.5	0.18	2.32	2.72 ± 0.32
473.2	4.5	0.48	6.43	2.70 ± 0.32
473.2	4.5	0.9	6.48	2.96 ± 0.32
473.2	4.5	1.76	11.43	2.97 ± 0.32
498.2	4.5	0.1	0.477	3.03 ± 0.31
498.2	4.5	0.2	1.05	2.99 ± 0.31
498.2	4.5	0.9	6.16	2.85 ± 0.33
523.2	4.5	0.1	0.247	3.20 ± 0.31
523.2	4.5	0.5	1.56	3.10 ± 0.31
523.2	4.5	0.9	2.9	3.07 ± 0.31

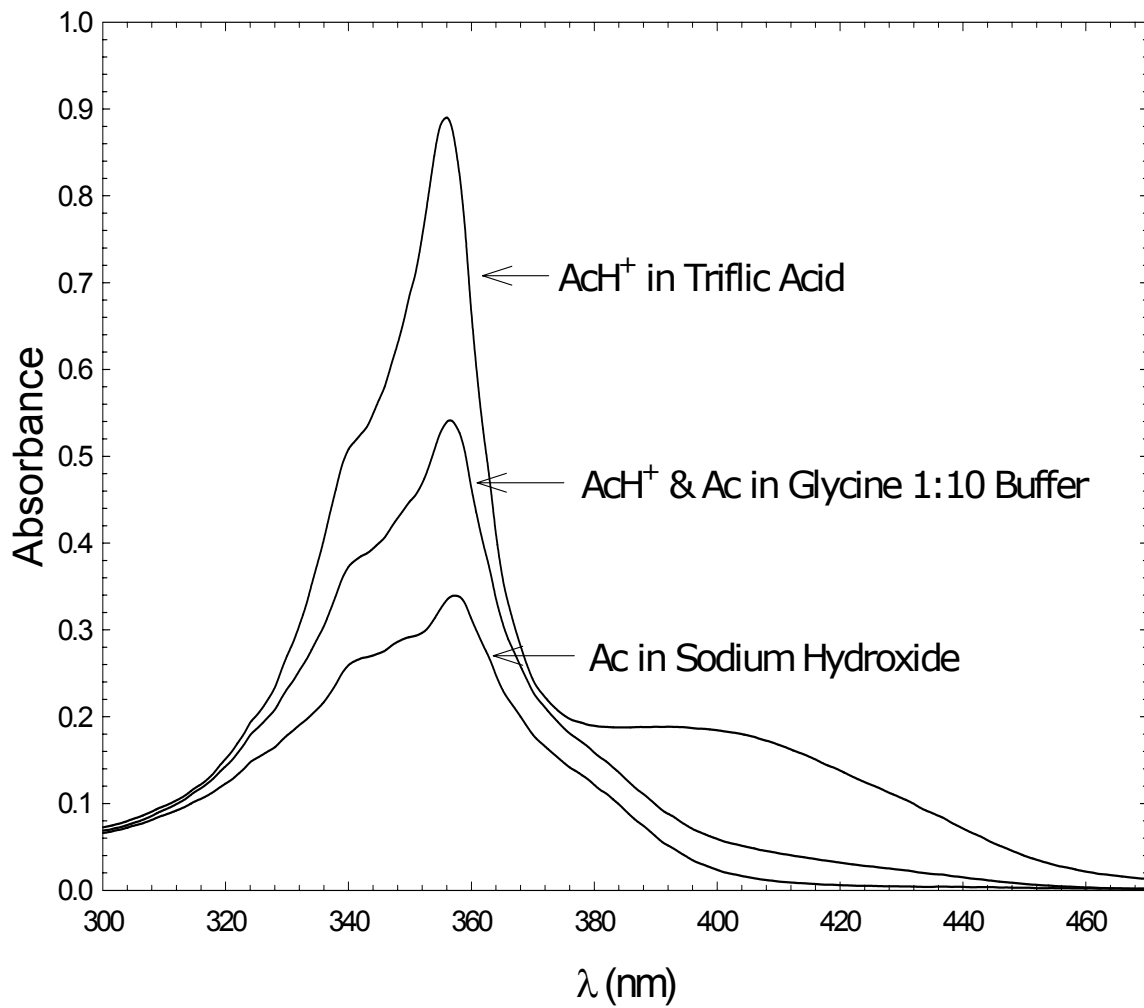


Figure 3.1.1.1 Absorbance spectra of acridine at 523.2 K in 0.0630 mol@g⁻¹ aqueous sodium hydroxide; 0.0345 mol@g⁻¹ triflic acid; and 0.0117 mol@g⁻¹ H₂A⁺ : 0.1331 mol@g⁻¹ HA[±] glycine buffer.

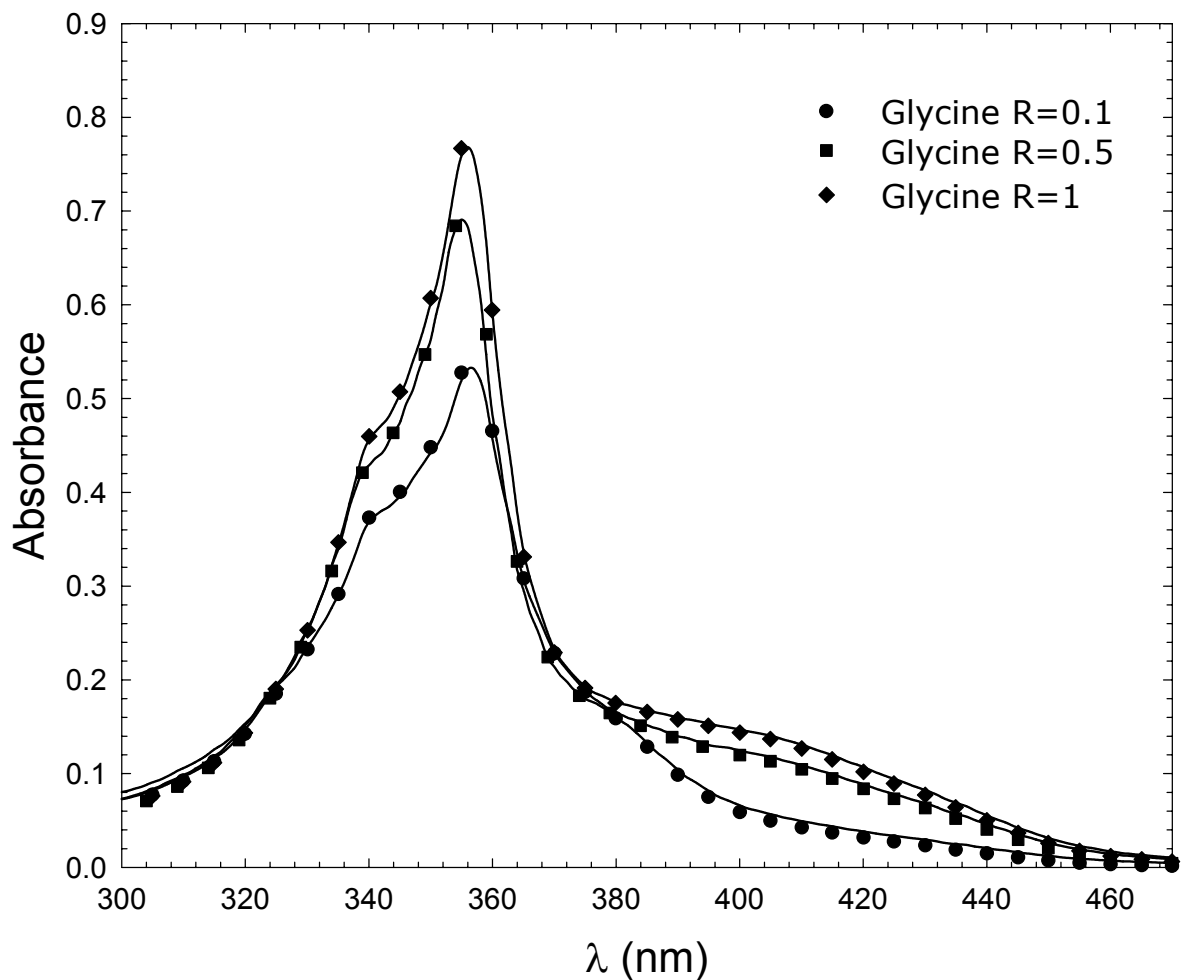


Figure 3.1.1.2 Absorbance of acridine at 523.2 K in aqueous glycine buffer solutions of varying $R = [\text{H}_2\text{A}^+] / [\text{HA}^\pm]$. Symbols represent experimental data. Solid lines represent fit to equation 2.3.1.1. Spectra of acridine in $0.0630 \text{ mol@g}^{-1}$ aqueous sodium hydroxide and $0.0345 \text{ mol@g}^{-1}$ triflic acid from Figure 3.1.1.1 were used to fit the data. For clarity, not all data points are shown.

3.1.2 Representation of Temperature Dependence of $\ln K_1$

Temperature dependence of stability constants can be expressed using the extended van't Hoff equation, given previously as 1.3.2.5:

$$\ln K_{T,P} = \ln K_{T_r, p_r} + \frac{\Delta_r H_{T_r, p_r}^{\circ}}{R} \left(\frac{1}{T_r} - \frac{1}{T} \right) + \frac{\Delta_r C_p^{\circ}}{R} \left(\ln \left(\frac{T}{T_r} \right) - 1 + \frac{T_r}{T} \right) \quad (3.1.2.1)$$

where T_r, p_r are the temperature and pressure of the reference state, $\Delta_r H_{T_r, p_r}^{\circ}$ is the standard partial molar enthalpy of reaction, and $\Delta_r C_p^{\circ}$ is the standard partial molar heat capacity of reaction. With a known value for $\ln K_{T_r, p_r}$ and a fixed T_r and p_r , values for $\ln K_{T,p}$ can be fit to equation 3.1.2.1 as a function of $1/T$ (K), with $\Delta_r H_{T_r, p_r}^{\circ} / R$ and $\Delta_r C_p^{\circ} / R$ as the fitting parameters. The values in Table 3.1.1.1 for pK_1 for glycine were converted to $\ln K_1$ and fit to equation 3.1.2.1, along with low temperature data from Wang *et al.* (1996), listed in Table 3.1.2.1. The reference value $\ln K_{1, T_r, p_r}$ was fixed to -5.400 at 298.15 K, 0.1 MPa from Wang *et al.* (1996). The resulting fit parameters are shown in Table 3.1.2.2 and the fit is plotted in Figure 3.1.2.1.

Table 3.1.2.1 Data from Wang *et al.* (1996)

T / K	pK_1
323.15	2.32
348.15	2.32
373.15	2.35
398.15	2.4

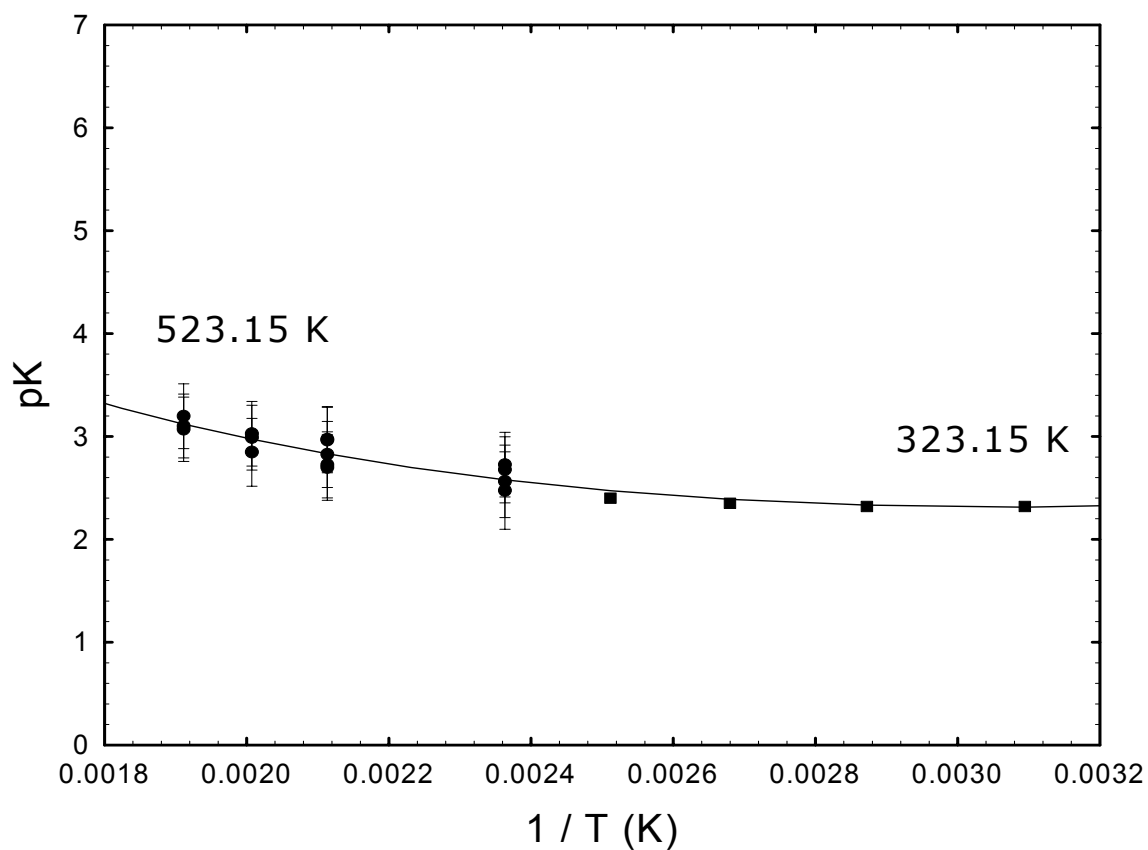


Figure 3.1.2.1 Temperature dependence of K_1 for glycine. ● This work; ■ Wang *et al.* (1996); solid line - fit to equation 3.1.2.1

Table 3.1.2.2 Values for fit of $\ln K_1$ to equation 3.1.2.1

Parameter	Value
$\ln K_{1,Tr,pr}$	-5.40
$\Delta_r H_{Tr,pr}^\circ$	$4315 \pm 1771 \text{ J mol}^{-1}$
$\Delta_r C_p^\circ$	$-159.7 \pm 18.3 \text{ J mol}^{-1} \text{ K}^{-1}$

3.2 Stability Constant K_2

3.2.1 Measurements Using 2-naphthol

Figure 3.2.1.1 compares the UV absorption spectra for 2-naphthol (2-nap) in triflic acid and 2-naphthol (2-nap) in sodium hydroxide with the spectrum of 2-naphthol in a buffer solution of glycine. Each UV-visible absorption spectrum represents an average of six scans taken over a period of approximately 15 minutes. K_2 of glycine is expected to fall within the indicator range for 2-naphthol at temperatures from 348.15 to 423.15 K. At each temperature of measurement in this interval, a baseline of the solution without 2-naphthol was subtracted from the spectrum of solution with 2-naphthol. As discussed in section 3.1.1, the spectra shown for the indicators in acid or base can be thought of as the extrema of a continuum from one form to the other. Because 2-naphthol concentrations varied slightly each day of experimentation and between solutions, absorbance in these spectra was normalized to a 2-naphthol concentration of $1.5 \times 10^{-4} \text{ mol kg}^{-1}$. Spectra of 2-naphthol in buffer solutions of glycine are expected to appear as intermediate between the extreme

spectra. This result was seen and is illustrated in Figure 3.2.1.1.

The 2-naphthol in glycine spectra were fit to equation 2.3.1.1 over the wavelength range 270nm - 400nm at intervals of 1nm. The spectra for 2-naphthol absorbance in several glycine buffer solutions of differing buffer ratios are shown as symbols in Figure 3.2.1.2. (Not all data points are shown, for clarity). The results of the fits to equation 2.3.1.1 for spectrum are plotted as solid lines in Figure 3.2.1.2. Values for K_4 were calculated for each buffer solution using equation 2.3.1.3. K_2 was then obtained by using $K_4 = K_2 / K_w$:

$$pK_2 = pK_4 + pK_w \quad (3.2.1.1)$$

Figure 3.2.1.2 shows spectra for a representative temperature; this process was repeated for all temperatures which were used in this work. The results are given in Table 3.2.1.1.

Table 3.2.1.1 Experimentally determined values of pK_2 as a function of temperature at 4.5 MPa using 2-naphthol indicator in glycine buffer solutions

T (K)	I (mol kg ⁻¹)	R [†]	$\frac{mA^-}{mHA^\pm}$	pQ_w^\ddagger	pK_4	pK_w^\ddagger	pK_2
323	0.0102	0.1	19.3	12.59	-3.71 ± 0.32	12.7	8.99 ± 0.32
323	0.0496	1	2.16	12.5	-3.74 ± 0.31	12.7	8.96 ± 0.31
323	0.0991	9.96	0.246	12.5	-3.73 ± 0.32	12.7	8.97 ± 0.32
373	0.0123	0.1	47.6	12.13	-3.78 ± 0.37	12.26	8.48 ± 0.37
373	0.0511	0.99	4.33	12.04	-3.73 ± 0.31	12.26	8.53 ± 0.31
373	0.1002	9.6	0.502	11.99	-3.72 ± 0.32	12.26	8.54 ± 0.32
398	0.0102	0.1	53.7	11.78	-3.57 ± 0.38	11.91	8.34 ± 0.38
398	0.0209	0.21	35.8	11.73	-3.71 ± 0.35	11.91	8.20 ± 0.35
398	0.0498	0.5	14.2	11.67	-3.68 ± 0.32	11.91	8.22 ± 0.32
398	0.0515	0.99	7.13	11.67	-3.68 ± 0.32	11.91	8.22 ± 0.32
398	0.1027	2.23	3.59	11.61	-3.74 ± 0.31	11.91	8.17 ± 0.31
398	0.0999	4.93	1.77	11.61	-3.76 ± 0.31	11.91	8.15 ± 0.31
398	0.1000	6.82	1.34	11.61	-3.76 ± 0.32	11.91	8.15 ± 0.32
398	0.1000	9.63	0.877	11.61	-3.69 ± 0.32	11.91	8.22 ± 0.32

[†] $R = m_{A^-} / m_{HA^\pm}$

[‡] Calculated from Sweeton *et al.* (1974).

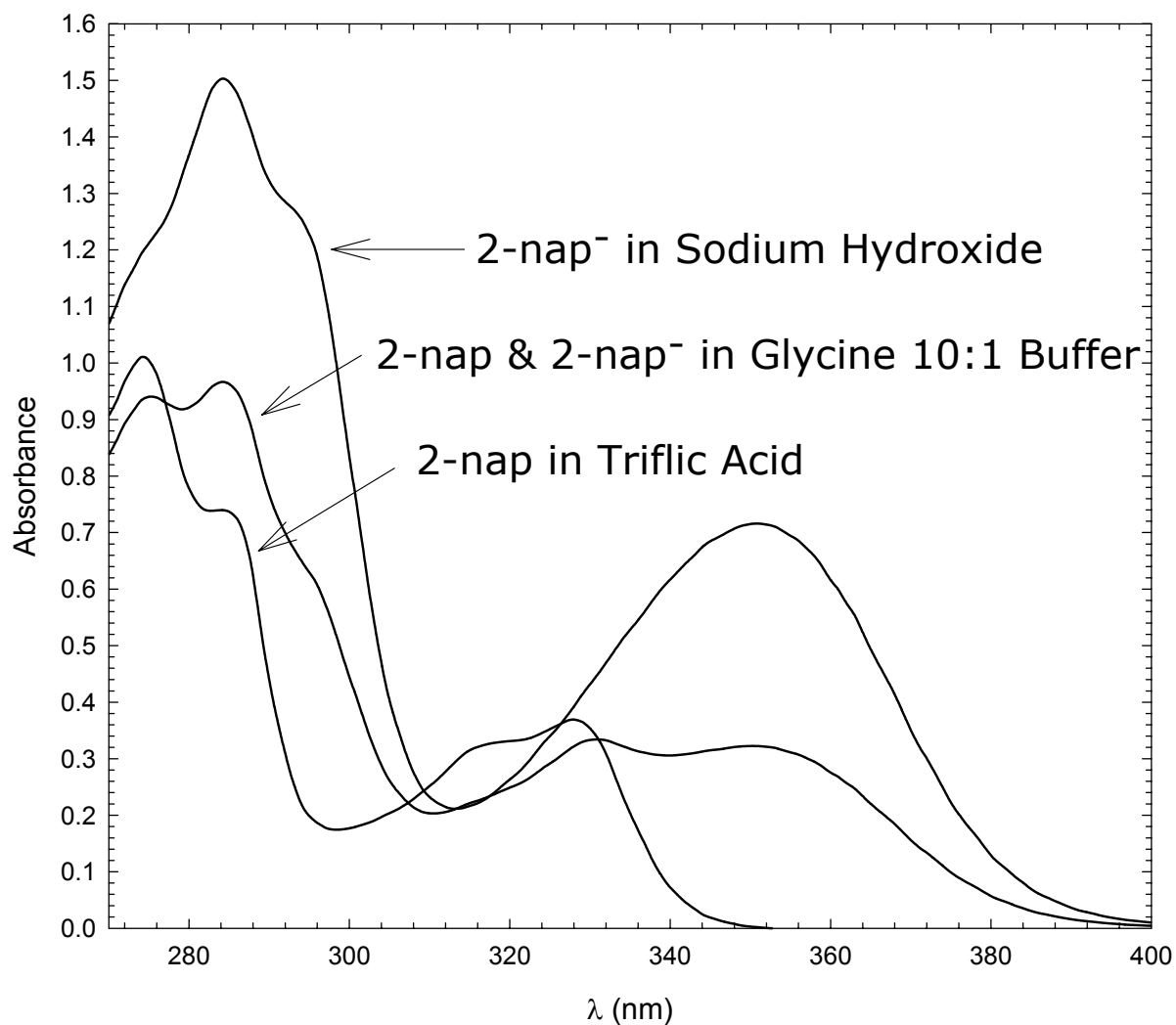


Figure 3.2.1.1 Absorbance spectra of 2-naphthol at 398.2 K in 0.1262 mol@g⁻¹ aqueous sodium hydroxide; 0.0803 mol@g⁻¹ aqueous triflic acid; 0.0982 mol@g⁻¹ A⁻ : 0.0102 mol@g⁻¹ HA[±] glycine buffer.

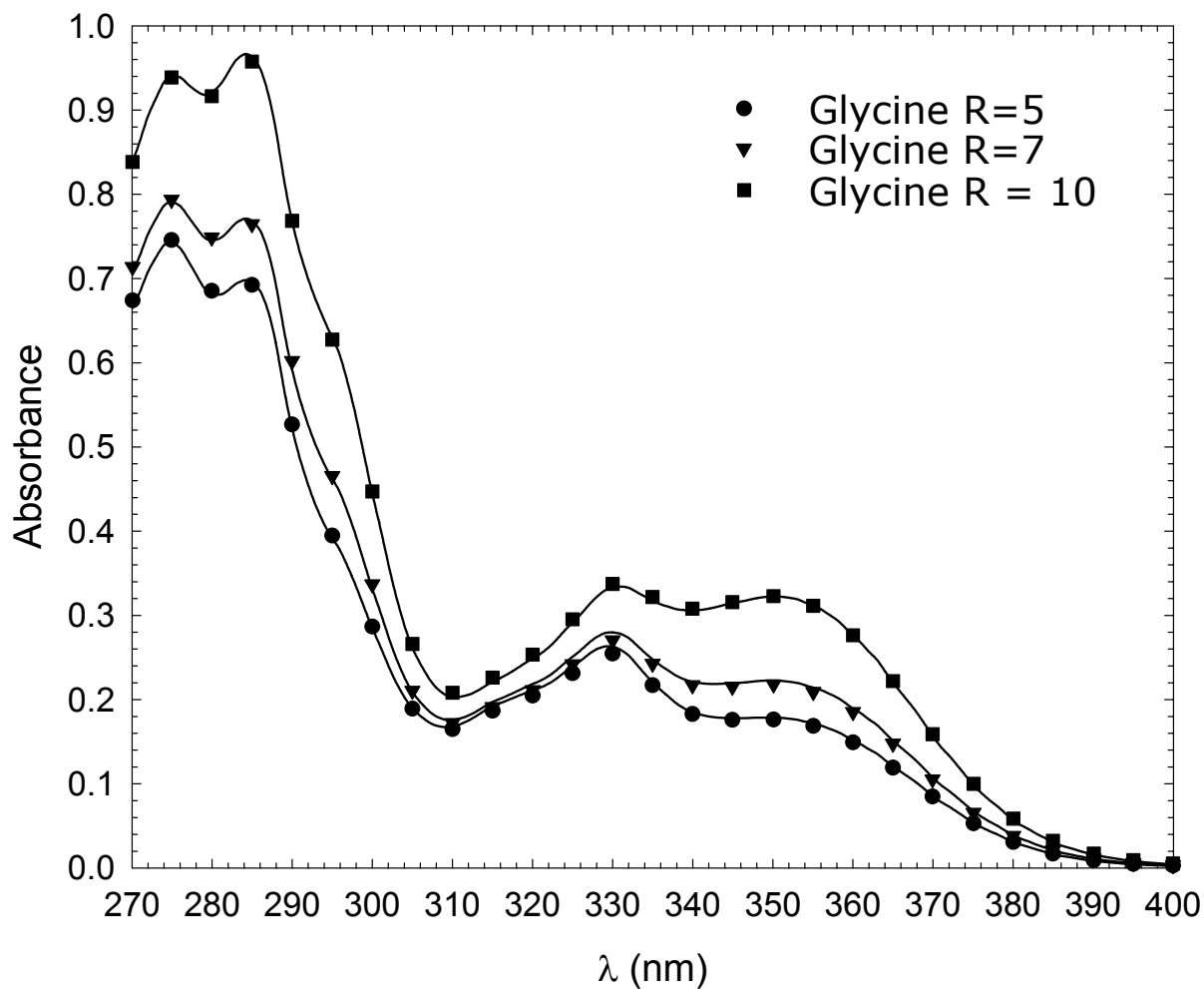


Figure 3.2.1.2

Absorbance of 2-naphthol at 398.2 K in aqueous glycine buffer solutions varying $R = m_{A^-} / m_{HA^+}$. Symbols represent experimental data. Solid lines represent fit to equation 2.3.1.1. Spectra of 2-naphthol in $0.1262 \text{ mol} \cdot \text{g}^{-1}$ aqueous sodium hydroxide and $0.0803 \text{ mol} \cdot \text{g}^{-1}$ aqueous triflic acid from Figure 3.2.1.1 were used to fit the data. For clarity, not all data points are shown.

3.2.2 Measurements Using 2-naphthoic Acid

As can be seen in Figure 1.4.2.2, 2-naphthoic acid is expected to be applicable for measurement of K_2 glycine at temperatures of 473.15 K - 573.15 K. Following the same method as was previously successful for acridine and 2-naphthol, 2-naphthoic acid was used with buffer solutions of glycine to measure K_2 at the temperatures of expected coincidence of K_2 and $K_{In, 2-naphthoic}$. Figure 3.2.2.1 shows a sample result in which the UV absorption spectra of 2-naphthoic acid in aqueous triflic acid and in aqueous sodium hydroxide are different. Because 2-naphthoic acid concentrations varied slightly each day of experiments and between solutions, absorbance in these spectra was normalized to a 2-naphthoic acid concentration of 1.5×10^{-4} mol kg⁻¹. Spectra of 2-naphthoic acid in buffer solutions of glycine are expected to appear as intermediate between the extreme pure acid and pure base spectra. This result was not seen. For all buffer ratios of glycine and at all temperatures of measurement from 473.15 K to 573.15 K the spectrum of 2-naphthoic acid in buffer appeared identical to that in sodium hydroxide, as seen in the example in Figure 3.2.2.1.

The 2-naphthoic acid in glycine spectra were fit to equation 2.3.1.1 over the wavelength range 270 nm - 400 nm at intervals of 1 nm. The result was as expected, showing almost completely deprotonated indicator in the buffer solutions. These results could not be used to calculate values for K_2 , but they show that pK_2 is higher than predicted by the

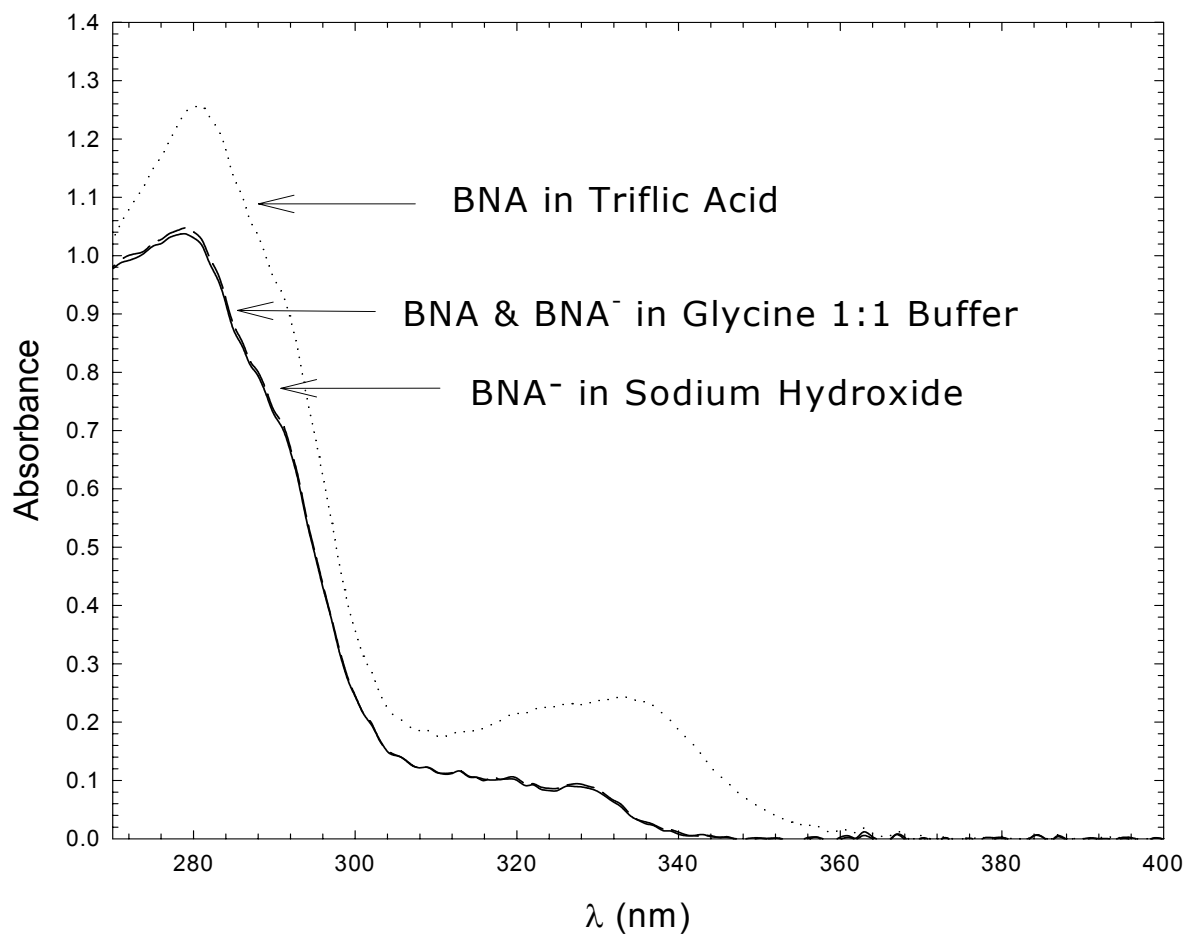


Figure 3.2.2.1

Absorbance spectra of 2-naphthoic acid at 498.2 K in 0.1212 mol@g⁻¹ aqueous sodium hydroxide; 0.0965 mol@g⁻¹ aqueous triflic acid; and 0.0500 mol@g⁻¹ A⁻ : 0.0494 mol@g⁻¹ HA[±] glycine buffer.

method of section 1.4.2 and must be at least equal to the upper limit of the indicator range. A lower limit has thus been established on pK_2 over the temperature range of measurement.

3.2.3 Representation of Temperature Dependence of $\ln K_2$

As was discussed previously, temperature dependence of stability constants can be expressed using the van't Hoff equation 3.1.2.1. For the glycine stability constant K_2 , this work has determined stability constants for 323.2 K # T # 398.3 K using 2-naphthol. Analysis of this data shows that it is best fit using the van't Hoff equation 3.1.2.1 with the term $)_r C_p^o / R$ set to zero. With a known value for $\ln K_{Tr,pr}$ fixed to 9.713 at 298.15 K, 0.1 MPa as given in Table 1.3.2.1, values for $\ln K_{T,p}$ can be fit to equation 3.1.2.1 as a function of $1/T$ (K), with $)_r H_{Tr,pr}^o / R$ as the fitting parameter. This method was applied to fit values of K_4 vs $1/T$. The resulting fitting parameters are given in Table 3.2.3.1. Using the expression for K_w given by Sweeton *et al.* (1974), K_2 can be calculated from K_4 . Figure 3.2.3.1 shows the data of this work and the fit line resulting from the fit to $\ln K_4$ and calculation of K_2 using K_w . Curvature is accounted for by curvature in the temperature dependence of K_w .

Table 3.2.3.1 Values for fit of $\ln K_4$ to equation 3.1.2.1

Parameter	Value
$\ln K_{4,Tr,pr}$	9.713
$)_r H_{Tr,pr}^o$	$-21817 \pm 1100 \text{ J mol}^{-1}$

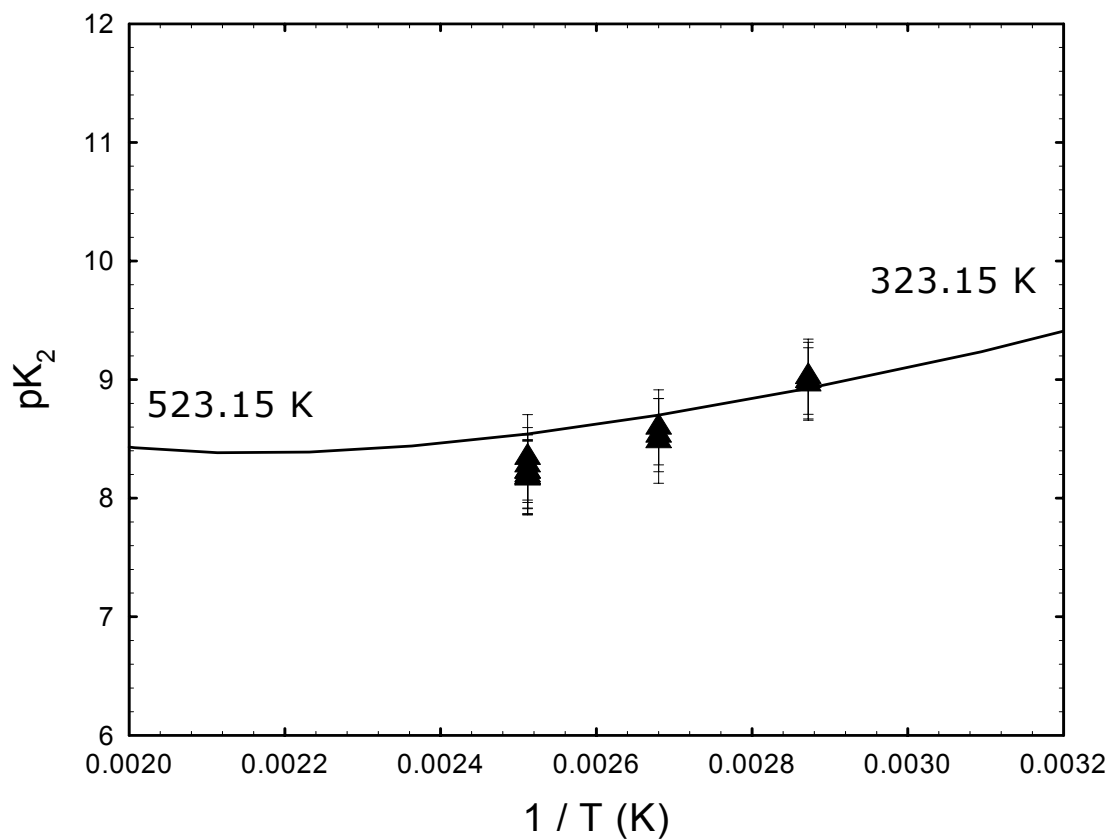


Figure 3.2.3.1 Temperature dependence of K_2 for glycine. Symbols represent experimental data, solid line represents fit to equation 3.1.2.1 to K_4 and conversion to pK_2 with equation 3.2.1.1.

3.3 Stopped-Flow Experiments

Two stopped-flow experiments were conducted to examine the stability of acridine absorbance over time. UV absorption spectra of acridine in a glycine 1:1 buffer containing $0.0316 \text{ mol} \cdot \text{g}^{-1} \text{H}_2\text{A}^+$ and $0.0350 \text{ mol} \cdot \text{g}^{-1} \text{HA}^\pm$ were taken at 523.2 K at 1.5 minute intervals for a period of 30 minutes. The first scan was started at the same time the flow was stopped. The resulting change in signal is illustrated in Figure 3.3.1. The acridine peak at 356nm decreased in intensity by 0.161 absorbance units, or 16% over the 30 minute run.

UV absorption spectra of acridine in a solution of $0.2560 \text{ mol} \cdot \text{g}^{-1}$ aqueous triflic acid were taken at 523.2 K at 1.5 min intervals for 30 minutes. The first scan, which began when the flow was stopped, was almost identical to that taken while flowing solution through the cell at $0.2 \text{ cm}^3 \cdot \text{min}^{-1}$. The acridine peak at 356nm decreased in intensity by 0.3897 absorbance units, or 39% over the 30 minute run. The change in absorbance with time is illustrated in Figure 3.3.2.

The greater loss of signal in triflic acid suggests a pH-dependent breakdown to acridine at 523.2 K, and not a breakdown of glycine. The experiment was repeated with triflic acid, measuring a spectrum at 0 minutes, placing the cell in darkness for 30 minutes, and recording a spectrum again. Signal loss of 39% was again seen, showing that the temperature and pH are greater factors in the breakdown of acridine than is exposure to light.

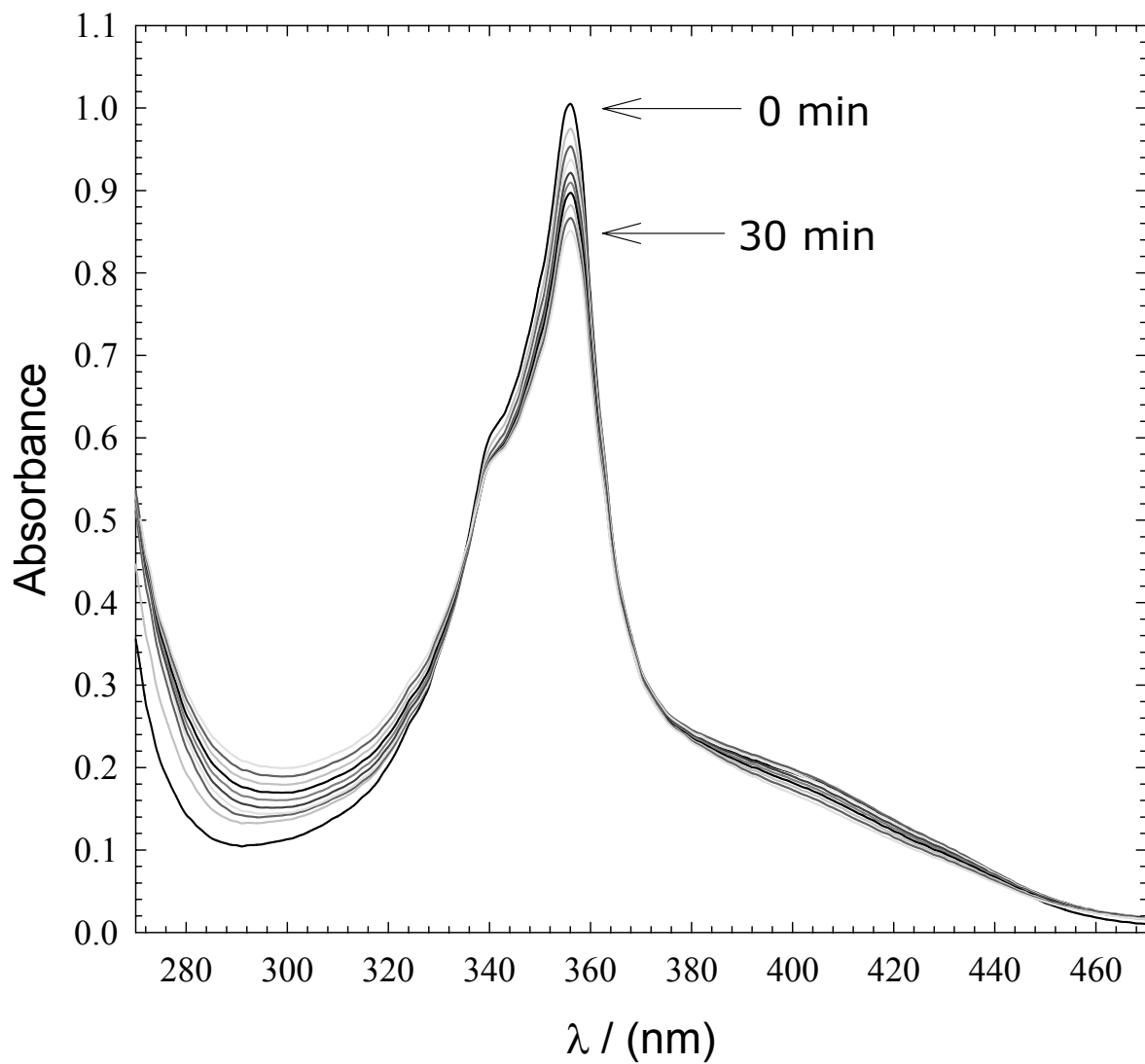


Figure 3.3.1 Change in absorbance of acridine at 523.2 K in aqueous $0.0316 \text{ mol} \cdot \text{g}^{-1} \text{H}_2\text{A}^+ : 0.0350 \text{ mol} \cdot \text{g}^{-1} \text{HA}^\pm$ glycine buffer over time.

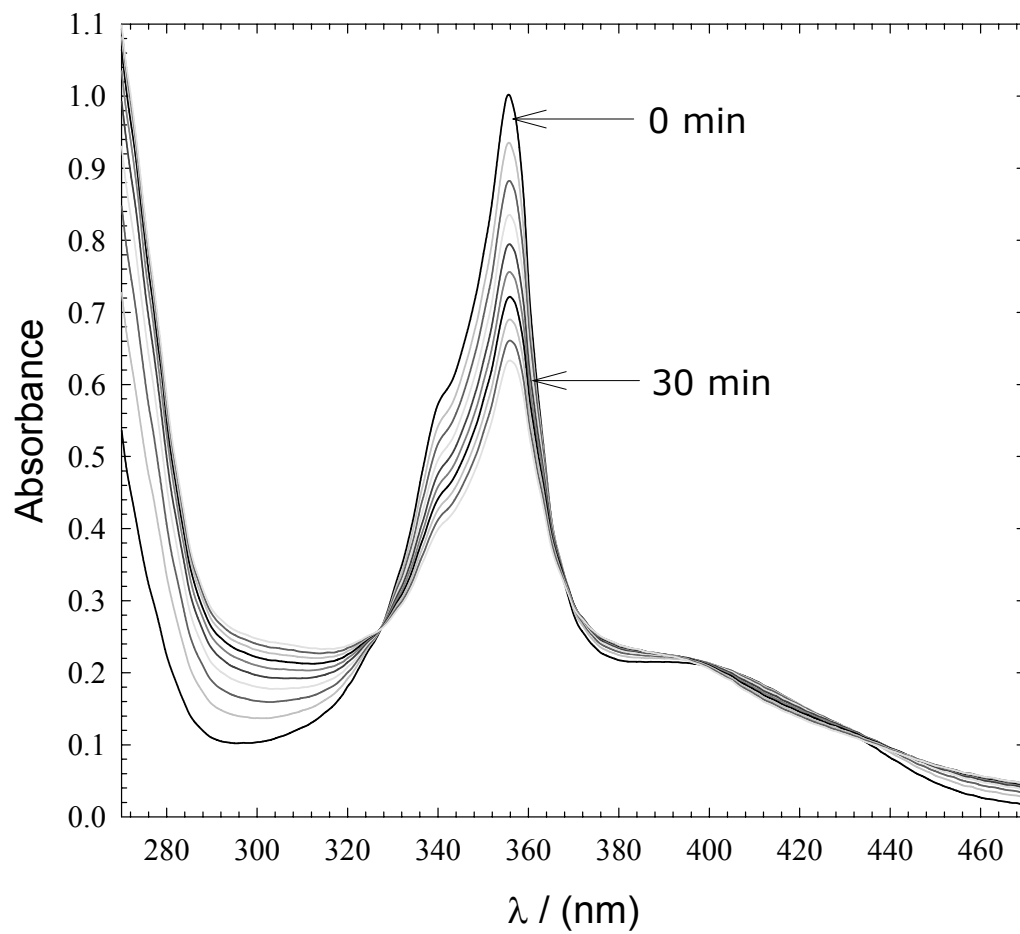


Figure 3.3.2 Change in absorbance of acridine at 523.15 K in 0.2560 mol@g⁻¹ aqueous triflic acid over time.

CHAPTER 4 - CONCLUSION

In this work K_1 and K_2 of glycine were measured using colorimetric indicators, and the temperature dependent relationships were extended into the hydrothermal region using the van't Hoff equation. In the region above 400 K, lower limits were obtained for pK_2 of glycine using 2-naphthoic acid as a colorimetric indicator. Experimental results show a good agreement with the stability constants predicted using extrapolation of room temperature thermodynamic data for K_1 . Experimental results for K_2 under hydrothermal conditions do not agree with those predicted using data at 298.15 K. The van't Hoff fit of K_4 calculated in this work gives values of pK_2 in good agreement with the experimental results both at room temperature and under hydrothermal conditions.

Acridine and 2-naphthol were used successfully as pH indicators for glycine dissociation equilibria. Results show that uncertainty is lower when the unknown spectrum is intermediate between the spectra of indicator in acid and indicator in base. Experimental uncertainty also depends on the relative differences between the spectra of indicator in acid and indicator in base. When these extreme spectra differ greatly, the uncertainty of fitting to equation 2.3.1.1 is minimized. Of the indicators studied, 2-naphthol gave the greatest difference between acidic and basic forms. When the spectrum of indicator in buffer strongly resembles either of the extreme spectra, as was the case with 2-naphthoic acid, stability constants cannot be calculated. In these cases, general inferences may be made

about the value of the stability constant. In this work, it was shown that pK_2 of glycine is greater than the upper limit of the indicator range of $pK_{2\text{-naphthoic acid}}$ at 475.2 # T # 523.2 K.

Stopped-flow studies of acridine stability over time at 523.2 K show that over the average residency time of solution in the flow cell (1.5 minutes), the signal loss is low (approximately 3% in 2 minutes) and within experimental error.

Further work in this study could include experiments to measure K_2 of glycine at high temperatures using 2-naphthol, as results with 2-naphthoic acid show pK_2 under hydrothermal conditions is more basic than predicted.

The hydrothermal properties of amino acids are of intense interest to many scientific disciplines, and may be important factors in theories of the origin of life at deep ocean hydrothermal vents. If solubilities are sufficient, stability constants for other amino acids and other acid/base buffer systems such as amine solutions under hydrothermal conditions can be measured using this process.

CHAPTER 5 - BIBLIOGRAPHY

Atkins P.W. (1990), *Physical Chemistry*. Fourth Edition; W.H. Freeman and Company: New York.

Bada J.L., Miller S.L., and Zhao M.X. (1995), The Stability of Amino Acids at Submarine Hydrothermal Vent Temperatures. *Origins of Life and Evolution of the Biosphere* **25**, 111-118.

Balakrishnan P.V. (1988), Liquid-Vapour Distribution of Amines and Acid Ionization Constants of Their Ammonium Salts in Aqueous Systems at High Temperature. *J. Sol. Chem.* **17**, 825-840.

Baross J.A. and Deming J.W. (1983), Growth of 'Black Smoker' Bacteria at Temperatures of at Least 250°C. *Nature* **303**, 423-426.

Chlistunoff J., Ziegler K.J., Lasdon L., and Johnston K.P. (1999), Nitric/Nitrous Acid Equilibria in Supercritical Water. *J. Phys. Chem.* **103**, 1678-1688.

Clarke, R. G. (2000), *Amino Acids Under Hydrothermal Conditions: Apparent Molar Volumes, Apparent Molar Heat Capacities, and Acid/Base Dissociation Constants For Aqueous L-Alanine, D-Alanine, Glycine, and Proline at Temperatures From 25 to 250°C and Pressures Up To 30.0 MPa*. Ph.D. Thesis, Memorial University of Newfoundland.

Martell A.E. and Smith R.M. (1974), *Critical Stability Constants. Volume 1: Amino Acids*. Plenum Press: New York.

Miller S.L. and Bada J.L. (1988), Submarine Hot Springs and the Origin of Life. *Nature* **334**, 609-611.

Ryan E.T., Xiang T., Johnston K.P., Fox M.A. (1997), Absorption and Fluorescence Studies of Acridine in Subcritical and Supercritical Water. *J. Phys. Chem.* **101**, 1827-1835.

Shock E.L. (1990), Do Amino Acids Equilibrate in Hydrothermal Fluids? *Geochim. Cosmochim. Acta.* **54**, 1185-1189.

Shock E.L. (1992), Stability of Peptides in High Temperature Aqueous Solutions. *Geochim. Cosmochim. Acta.* **56**, 3481-3491.

Spies F.N., MacDonald K.C., Atwater T., Ballard R., Carranza A., Cordoba D., Cox C., DiazGarcia V.M., Francheteau J., Guerrero J., Hawkins J., Haymon R., Hessler R., Juteau T., Kastner M., Larson R., Luyendyk B., MacDougall J.D., Miller S., Normark W., Orcutt

- J., Rangin C. (1980), East Pacific Rise: Hot Springs and Geophysical Experiments. *Science* **207**, 1421-1433.
- Sweeton F. H., Mesmer R. E. , and Baes C. F. Jr. (1974), Acidity Measurements at Elevated Temperatures. VII. Dissociation of Water. *J. Sol. Chem.* **3**, 191-214.
- Trent J.D., Chastain R.A., and Yayanos A.A. (1984), Possible Artefactual Basis for Apparent Bacterial Growth at 250°C. *Nature* **307**, 737-740.
- Trevani L.N., Roberts J.C., and Tremaine P.R. (*submitted*), Copper(II)-Ammonia Complexation Equilibria in Aqueous Solutions at Temperatures from 30 to 250°C by Visible Spectroscopy.
- Vallentyne J.R. (1964), Biogeochemistry of Organic Matter - II. Thermal Reaction Kinetics and Transformation Products of Amino Compounds. *Geochim. Cosmochim. Acta.* **28**, 157-188.
- Wang P., Oscarson J.L., Gillespie S.E., Izatt R.M., and Cao H. (1996), Thermodynamics of Protonation of Amino Acid Carboxylate Groups from 50 to 125 °C. *J. Sol. Chem.* **25**, 243-265.
- Xiang T. and Johnston K.P. (1994), Acid-Base Behavior of Organic Compounds in Supercritical Water. *J. Phys. Chem.* **98**, 7915-7922.
- Xiang T. and Johnston K.P. (1997), Acid-Base Behavior in Supercritical Water: \$-Naphthoic Acid - Ammonia Equilibrium. *J. Solution Chem.* **26**, 13-30.
- Xiang T. (1996), *Spectroscopic Studies of Acid-Base Behavior in Supercritical Water*. Ph.D. Thesis; University of Texas at Austin.